



Paleoenvironmental reconstruction of the Middle Jurassic rocks in western India using benthic foraminifera

Sreepat Jain¹ · Mohamad Alhussein² · Mohamed S. Ahmed³ · Ahmed Awad Abdelhady^{2,4} 

Received: 13 January 2023 / Accepted: 7 May 2023 / Published online: 12 June 2023
© Springer-Verlag GmbH Germany, part of Springer Nature 2023

Abstract

The Middle Jurassic (Bajocian–Callovian) benthic foraminifera in the Jhura Dome (Kachchh, Western India) were quantitatively analyzed to reconstruct the paleoenvironment. Three distinct assemblages are identified; these are dominated by a particular benthic foraminiferal species, and include, the moderately mesotrophic and well-oxygenated *Protomarssonella poddari*, moderately mesotrophic and moderately oxygenated *Lenticulina subalata*, and the highly mesotrophic and moderately oxygenated *Epistomina mosquensis*–*Reophax metensis*. Based on species bathymetry, an inner to middle neritic (50–100 m) depth range is inferred for the studied section. The Bathonian is marked by a carbonate-dominated moderately mesotrophic regime, whereas the Callovian is siliciclastic-dominated and reflects highly mesotrophic conditions. The changes in facies and the trophic regime are attributed to a change in climate from a hot and drier Bathonian to a cooler and wetter Callovian with a progressive increase in the terrigenous input (= nutrient input) and in reduced oxygenation of bottom waters. The Canonical Correspondence Analysis yielded sea level, Benthic Foraminiferal Oxygen Index (BFOI) and paleoproductivity as the main factors controlling the distribution patterns of the studied benthic foraminifera. Additionally, within a shallow epeiric basin and in moderately to well-oxygenated bottom water conditions, the role of nutrients and oxygen availability overrides the influence of bathymetry that at the deeper settings, played a far greater role.

Keywords Benthic foraminifera · Paleooxygenation · Paleoproductivity · Paleoenvironment · Middle Jurassic · Kachchh

Introduction

The benthic foraminifera have been used, both quantitatively and qualitatively, to interpret past and present environments, bathymetry, productivity and oxygenation patterns, besides others, by using their abundance patterns, distinctive assemblages, test shapes (morphogroups), life-habits and their preference for oxygen availability (Corliss 1985; Bernhard 1986; Corliss and Chen 1988; Kaminski 1987; Nagy 1992;

Jorissen et al. 1995, 2007; Van der Zwaan et al. 1999; Nagy et al. 2000, 2013; Jain and Collins 2007; Jain et al. 2007, 2019, 2020; Kaminski et al. 2008, 2010; Reolid et al. 2013, 2015; Farouk and Jain 2016; Rita et al. 2016; Wolfgring and Wagneich 2016; Jain and Abdelhady 2020). These biotic parameters, at times together with abiotic ones (substrate type, clay mineralogy, stable isotopes, and sequence stratigraphy), have further enabled more precise assessment of varied Jurassic environments (Gebhardt et al. 2004; Jain et al. 2007, 2020; Reolid 2014; Farouk and Jain 2016, 2017; Rita et al. 2016; Nagy 2016; Jain and Farouk 2017; Farouk et al. 2020; Kaminski et al. 2020).

Recently, the variability in the distribution patterns of the Middle Jurassic (Bathonian–Callovian) benthic foraminifera were quantitatively analyzed from deeper waters (largely outer neritic and carbonate-dominated; Jumara Dome) from the depocenter of the Kachchh Basin, India (Jain et al. 2019; Wasim et al. 2021) (Fig. 1). Quantitative results suggested that the distribution patterns of benthic foraminifera were controlled by changes in sea level, oxygenation, and substrate type (sediment). Jain et al. (2019) also noted that the

✉ Ahmed Awad Abdelhady
ahmed.abdelhady@mu.edu.eg

¹ Department of Geology, School of Applied Natural Science, Adama Science and Technology University, Oromia, 1888 Adama, Ethiopia

² Department of Palaeontology, University of Vienna, Althanstrasse 14, 1090 Vienna, Austria

³ Geology and Geophysics Department, College of Science, King Saud University, 2455, Riyadh 11451, Saudi Arabia

⁴ Department of Geology, Faculty of Science, Minia University, El Minia 61519, Egypt

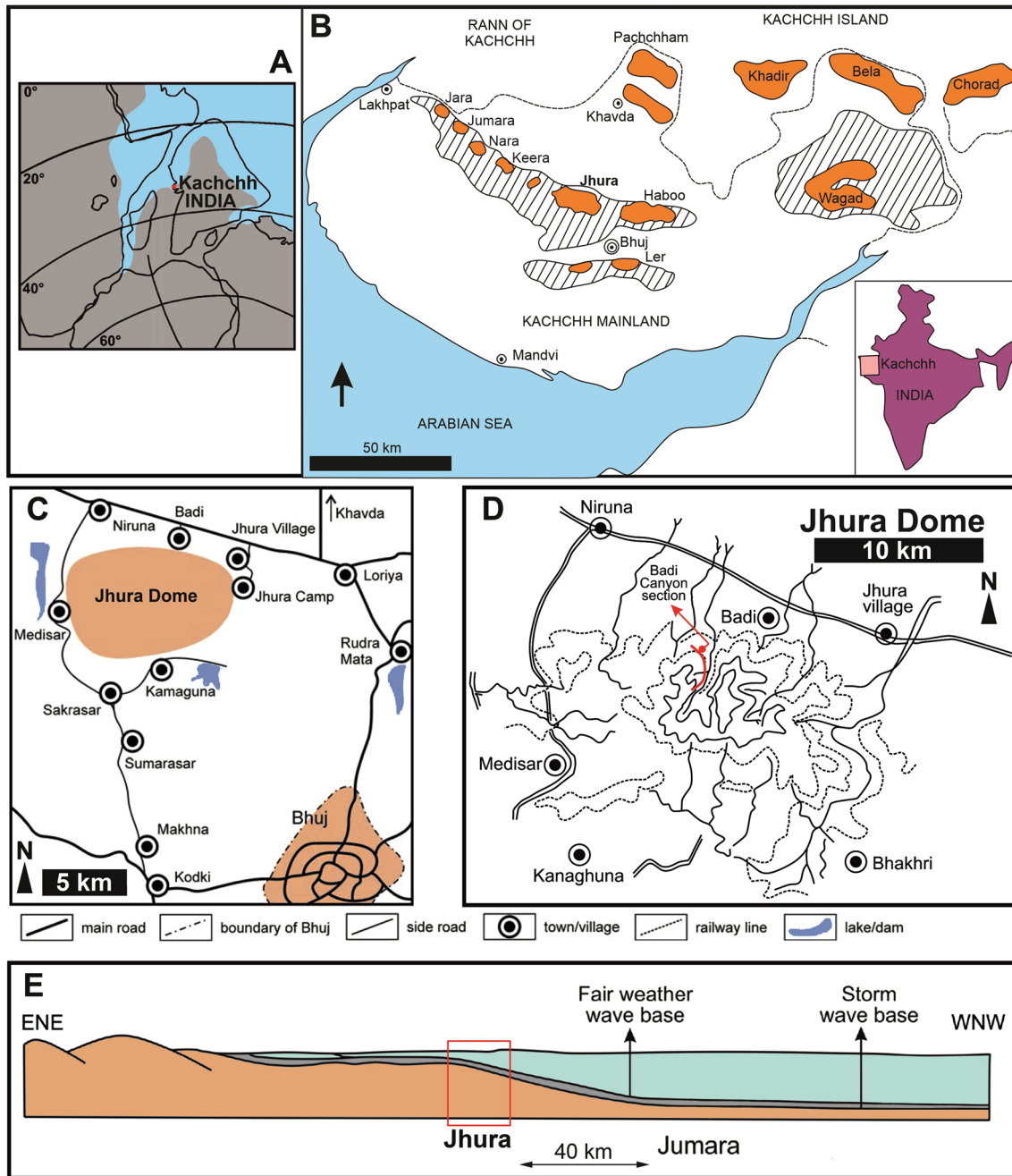


Fig.1 Kachchh (western India) and Jhura Dome. **A** Palaeogeographic map showing the position of India and Kachchh (modified after Enay and Cariou 1997). Shaded area: land. **B–C** Jurassic localities exposed within the Kachchh Basin and the location of the Jhura Dome (C).

D Map of Jhura Dome modified after Fürsich et al. (2014), red line refers to the studied section. **E** Depositional setting of Jhura and Jumara (modified after Fürsich 1998)

taxa with specific biotic traits such as shell composition (calcareous vs agglutinated), and selection strategy (r- vs k-strategy) occupied distinctly different (and statistically significant) environmental settings. The assertion by Jain et al. (2019) that sea level-controlled sedimentation patterns, which in turn, governed trophic resources within the Kachchh Basin has been noted by other studies, as well

(Olóriz et al. 2003, 2012), and has also been recently corroborated by another quantitative data from the marginal mixed-siliciclastic Callovian-Oxfordian rocks of Ler, Kachchh, western India (Wasim et al. 2020, 2021) (see Fig. 1B for locality).

We present here the highest resolution study from the Jurassic rocks of Kachchh (western India) based on 48

samples containing 443,131 specimens. This study quantitatively analyzes the distribution patterns of the Bajocian to Callovian (Middle Jurassic) benthic foraminifera from a largely inner neritic and siliciclastic-dominated depositional setting of the Jhura Dome (Kachchh) (Fig. 1). The present study also aims to add to the much-needed quantitative body of work within the scarce Middle Jurassic time on the distribution patterns of benthic foraminifera from shallower siliciclastic settings (Canales et al. 2014), that has so far largely been accessed through qualitative and/or semi-quantitative methods (Nagy 1985, 2016; Nagy et al. 1995, 2001, 2010a, b; Reolid and Martínez-Ruiz 2012; Reolid et al. 2008a, b, 2019; Kaminski et al. 2020).

This study, tests three hypotheses:

- (1) What are the major biotic/abiotic factors controlling the distribution patterns of benthic foraminifera in shallow siliciclastic-dominated marine ecosystems?
- (2) Is there a temporal shift in the patterns of benthic foraminiferal species/assemblages between the deeper carbonate-dominated (Jumara Dome; Jain et al. 2019) and the shallow siliciclastic-dominated (Jhura Dome; this study) settings?
- (3) Can the inferred changes in the benthic foraminiferal distribution patterns be significantly correlated to specific biotic/abiotic parameters?

Additionally, and based on quantitative analyses, an attempt is also made to rank the role of both abiotic (e.g., sea level, oxygenation, nutrients, and substrate type) as well

as biotic (life-habit, shell composition, species diversity) parameters in shaping the benthic foraminiferal distributional patterns for the studied Bajocian–Callovian interval.

Previous work

The distribution patterns of benthic foraminifera recorded from the Jurassic rocks of the Kachchh Basin have not yet been fully investigated with proper sampling rigor (Table 1). Those that have been done are based on meagre samples with very few specimens (Table 1) and are largely restricted to documenting basic taxonomy (addressed by Alhussein 2010, 2014), or inferring broad paleoenvironmental basinal conditions (open marine or restricted/deep or shallow basinal settings) (see Table 1). Besides low-resolution sampling, poor biostratigraphic constraints and a complete lack of a multiproxy approach have often led to large inconsistencies and contradictions in the inference of the paleoenvironment. This study applies a multiproxy approach to infer changes in the paleoenvironment, but also compares data with the depositor of the basin, Jumara Dome, for a basin-wide analysis.

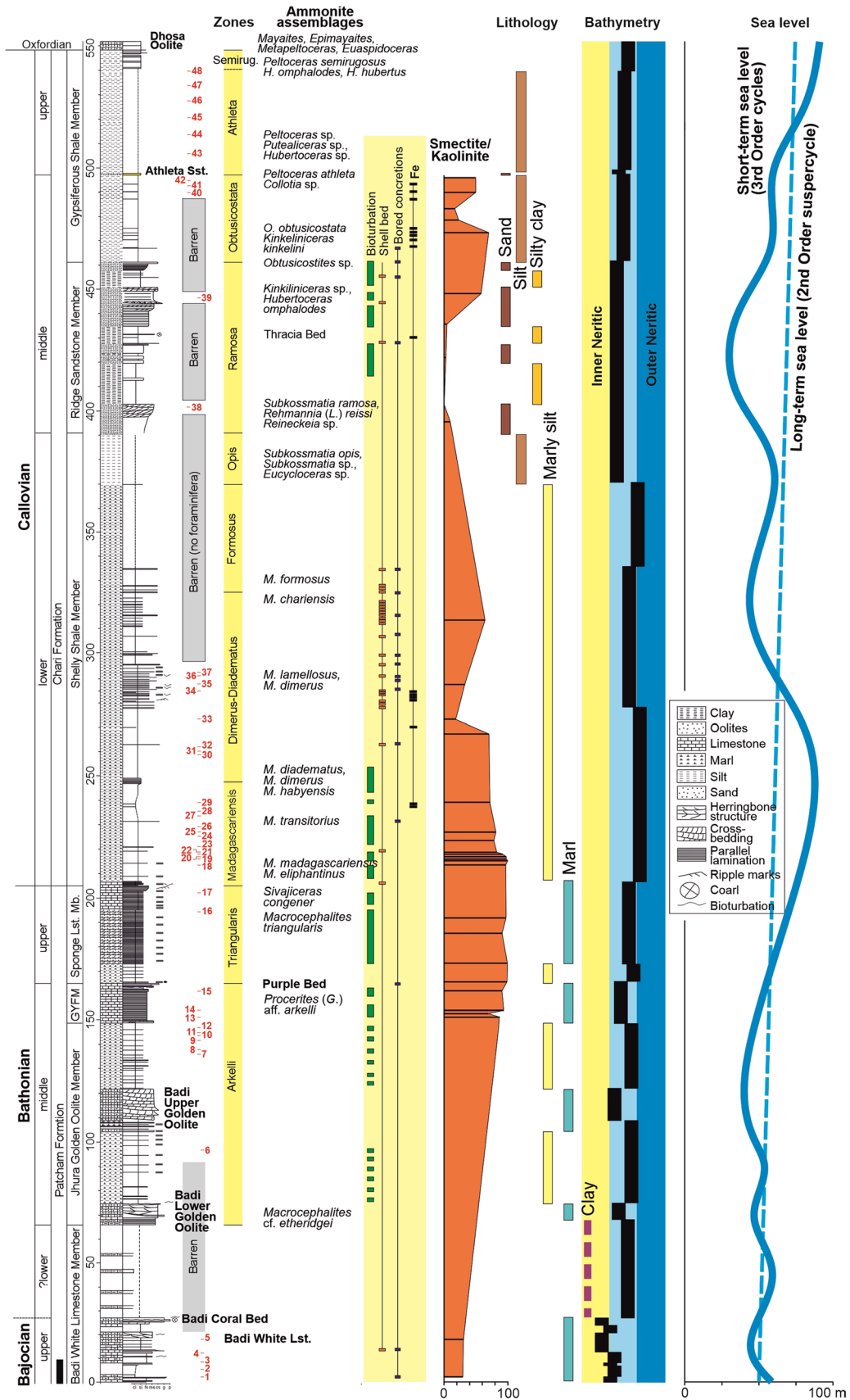
Geological setting

The Jhura Dome (23° 26' 8" N, 69° 37' 00" E; Kachchh Basin) (Fig. 1) exposes 550 m thick Middle Jurassic (upper Bajocian to early-middle Oxfordian) sediments; the upper Bajocian–upper Callovian is the studied interval (Fig. 2).

Table 1 Previous work

References	Locality	No. of samples	Specimens per sample
Bhalla and Talib (1985a, b)	Jhura	28	Not given
Bhalla and Talib (1991)	Jhura	28	Semi-qualitative; Rare = 1–3 specimens; Frequent = 4–6 specimens; Abundant = > 7 specimens
Bhalla et al. (1998a, b)	Jhura	Not given	Not given
Gaur and Singh (2000)	Nara	30	Semi-qualitative; Rare = 1–3 specimens; Frequent = 4–6 specimens; Abundant = > 7 specimens
Talib and Bhalla (2006)	Jhura	Not given	Not given
Talib and Faisal (2007)	Ler	Not given	Not given
Talib et al. (2007)	Jumara, Jhura	6, 10 (respectively)	Semi-qualitative; Rare = 1–3 specimens; Frequent = 4–6 specimens; Abundant = > 7 specimens
Gaur and Talib (2009)	Jumara	18	
Talib et al. (2012a)	Kaiya	27	
Talib et al. (2012b)	Keera	16	
Talib et al. (2016)	Habo	10	Semi-qualitative; Rare = 1–5 specimens; Frequent = 5–9 specimens; Abundant = > 10 specimens
Talib et al. (2017)	Keera	21	8
Wasim et al. (2020)	Ler	43	% Frequency data (specimens categorized as < 1, 1–5, 5–10, 10–20, 20–50 and > 50)
This study	Jhura	86	5152 specimens/sample

Note the low sample numbers. Figure 1 shows the mentioned localities



◀**Fig. 2** Jhura Dome section showing sample placement, ammonite biozonation, vertical distribution of bioturbated sediments, shell beds, bored concretions, Fe-rich beds, trace fossils, smectite/kaolinite ratio, lithology, bathymetry, and inferred relative sea level (this study). The Smectite/Kaolinite ratio is after Fürsich et al. (2005). See text for further explanation

The sediments are largely made up of siliciclastics with minor carbonates at the base, constituting the ~200 m thick Bajocian–Bathonian carbonate-dominated Patcham Formation and followed by the ~350 m thick siliciclastic-dominated Callovian Chari Formation (Fig. 2) (for age determination see Roy et al. 2007; Jain 2014, 2020).

The Patcham Formation is divided into four members (from base to top): Badi White Limestone, Jhura Golden Oolite, Goradongar Yellow Flagstone and Sponge Limestone (Fig. 2). The succeeding Chari Formation also has four members, Shelly Shale, Ridge Sandstone, Gypsiferous Shale and Dhosa Oolite (Fig. 2). The lithostratigraphy used here is modified after Fürsich et al. (2001) and Fürsich et al. (2014). The topmost Dhosa Oolite Member was not sampled; it is a heavily bioturbated clayey, fossil-rich, condensed Fe-oolitic limestone, with abundant wood fragments and records the maximum flooding of the basin during the early-middle Oxfordian interval.

The Badi White Limestone Member (BWL) consists mainly of 66 m white bioturbated clayey to oolitic limestones. The primary sedimentary structures include wave ripples, smaller ones in the basal part, and larger ones at the top (Fig. 2). The succeeding Jhura Golden Oolite Member (JGOM) is about 84 m and has two Fe-oolitic sandy limestone units, the Badi Lower Golden Oolite (BLGO) and the Badi Upper Golden Oolite (BUGO) (Fig. 2). The lithology above and below the BUGO, is composed of silty marls with thin and fine-grained parallel-laminated sandstone intercalations (Fig. 2). The characteristic lower middle Bathonian Indonesian *Macrocephalites* cf. *etheridgei*, and also earliest ammonite was recorded from the BLGO (Roy et al. 2007; see also Jain 2014, 2019, 2020). The succeeding Goradongar Yellow Flagstone Member (GYFM) consists of 15 m silty marls with thin limestone interbeds (Fig. 2). The upper part is made up of thin-bedded bioturbated limestones, that occasionally contain iron-crusts. The GYFM is topped by a sharp erosional contact with the overlying Purple Sandstone bed, a purple-colored fossil-rich sandstone (Fig. 2). The erosive base of this bed is possibly a sequence boundary and the bed, itself, a Maximum Flooding Surface (MFS) (see also Fürsich et al. 2001). The GYFM has yielded another characteristic lower middle Bathonian ammonite, *Procerites* (*Gracilisphinctes*) aff. *arkelli* (see Jain et al. 1996; Jain 2019) (Fig. 2). The overlying ~50 m thick Sponge Limestone Member (SLM) is about 42 m of bioturbated silty marls with abundant interbeds of parallel laminated and graded

packstones (limestones) (Fig. 2). The topmost part of this unit has parallel laminated, thin-bedded and fossil-rich (bivalves and brachiopods; see Fürsich et al. 2014) sandy limestones that show nodular morphology, quite characteristic of SLM, and noted across the basin; SLM is a marker bed (see Jain 1996, 2014, 2020; Jain et al. 1996; Fürsich et al. 2001, 2014).

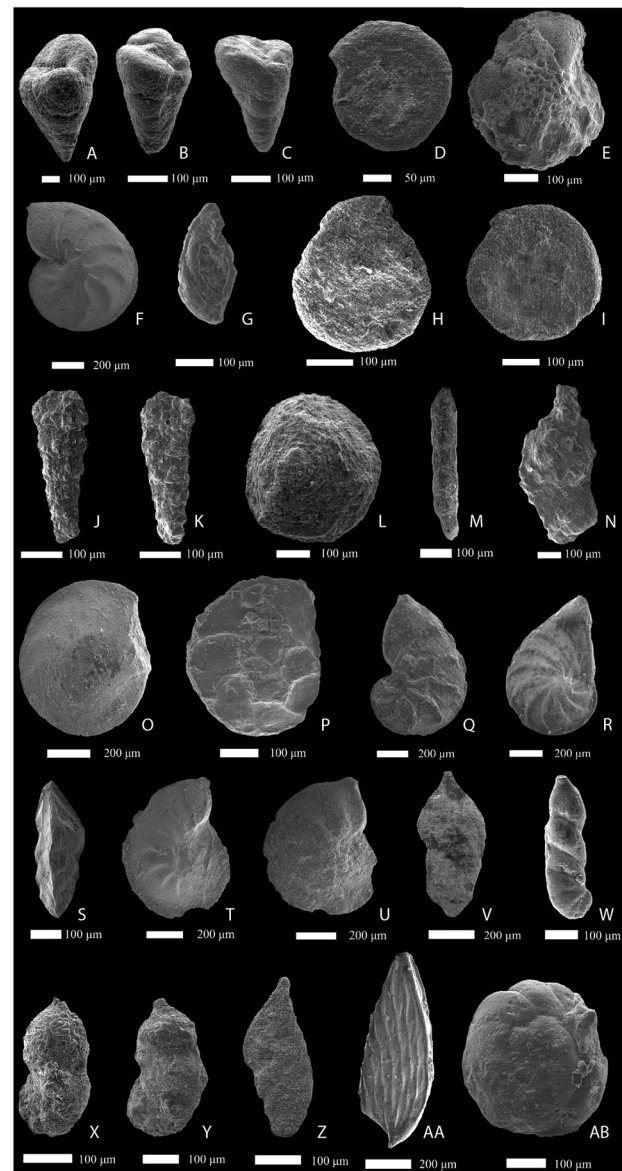
The succeeding ~340 m thick Chari Formation has four members (from base to top)—Shelly Shale, Ridge Sandstone, Gypsiferous Shale and Dhosa Oolite (Fig. 2). Fürsich et al. (2001) added another member, below the Dhosa Oolite, the Dhosa Sandstone Member (DSM). The topmost lower middle Oxfordian Dhosa Oolite Member has not been sampled in the present contribution (Fig. 2). The Shelly Shale Member (SSM) is 195 m of bioturbated sandy marl unit characterized by more silty content in its middle and upper parts. The middle part is very rich in fossils, with shells mostly concentrated as thin layers that contain abundant bored and encrusted concretions; the well-preserved shells are rarely fragmented. The succeeding Ridge Sandstone Member (RSM) consists of massive sandstones with silty interbeds (Fig. 2). The sandstone is characterized by large-scale trough-cross-bedding, whose top is Fe-encrusted. Its upper part is dominantly composed of fine-sands to bioturbated fossil-rich silty sandstones with shell beds.

The ammonite biostratigraphy used in this study (Fig. 2) is based on field observations by one of us (SJ) and after Roy et al. (2007), and in comparison, with the adjoining Jumara Dome, the depocenter of the basin (after Jain 1996, 2014, 2019, 2020). The latter zonation is based on the presence of index forms coeval with those occurring within the Sub-mediterranean and European standard ammonite zones (Jain 1996, 2014, 2019, 2020; Jain et al. 2019) (Fig. 2).

Materials and methods

A total of 48 samples were analyzed that yielded 443,131 benthic foraminifera specimens from 200 g of material (Fig. 2). The material was disaggregated using 10% hydrogen peroxide and washed through 63 µm, 125 µm, 250 µm and 500 µm mesh sieves. After drying the residue, the samples were picked from the > 125 µm fraction (Alhussein 2010, 2014). The benthic foraminiferal samples were placed (as precisely as possible) within the updated ammonite zones (Roy et al. 2007; Jain 2014) of the studied section (see Fig. 2). The taxonomy of picked benthic foraminifera has already been dealt with and published by one of us (Alhussein 2014). Representative benthic foraminiferal species are illustrated in Fig. 3. The studied material is deposited at the Bavarian Julius Maximilians University of Würzburg (Würzburg, Germany).

Fig. 3 Dominant foraminifera species: **A** *Protomarssonella poddari* ▶ (Subbotina, Datta and Srivastava); bed 1, *Protomarssonella poddari*–*Protomarssonella prekummi* Assemblage, late Bajocian. **B–C** *Protomarssonella prekummi* Pandey and Dave, 1993; bed 16, *Spirillina polygyrata* Sub-assemblage, upper Bathonian. **D** *Spirillina polygyrata* Guembel, 1862, bed 12, *Spirillina polygyrata* Sub-assemblage, upper Bathonian. **E** *Epistomina alveolata* Myatliuk, 1954, bed 12, *Spirillina polygyrata* Sub-assemblage, upper Bathonian. **F** *Lenticulina muensteri* (Roemer, 1839), bed 40, *Lenticulina muensteri* Sub-assemblage, middle Callovian. **G** *Triloculina* sp., bed 40, *Lenticulina muensteri* Sub-assemblage, middle Callovian. **H–I** *Ammodiscus asper* (Terquem, 1862); bed 16, *Spirillina polygyrata* Sub-assemblage, upper Bathonian. **J–K** *Ammobaculites hagni* Bhalla and Abbas, 1978; Bed 45, *Epistomina mosquensis*–*Reophax metensis* Assemblage, upper Callovian. **L** *Trocholina conosimilis* Subbotina, Datta and Srivastava, 1960, bed 22, *Protomarssonella prekummi* Sub-assemblage, lower Callovian. **M** *Lingulina laevissima* (Terquem, 1866), bed 2, *Protomarssonella poddari*–*Protomarssonella prekummi* Assemblage, late Bajocian. **N–O** *Reophax metensis* Franke, 1936, bed 48, *Epistomina mosquensis*–*Reophax metensis* Assemblage, upper Callovian. **P** *Epistomina preventriosa* Pandey and Dave, 1993, bed 44, *Epistomina mosquensis*–*Reophax metensis* Assemblage, upper Callovian. **Q** *Epistomina mosquensis* Uhlig, 1883, bed 44, *Epistomina mosquensis*–*Reophax metensis* Assemblage, upper Callovian. **S** *Lenticulina quenstedtii* (Gümbel, 1862), bed 30, *Protomarssonella prekummi* Sub-assemblage, lower Callovian. **T** *Lenticulina subalata* (Reuss, 1863), bed 30, *Protomarssonella prekummi* Sub-assemblage, lower Callovian. **U** *Tribrachia inelegans* Loeblich and Tappan, 1943, bed 20, *Spirillina polygyrata* Sub-assemblage, upper Bathonian. **V** *Lenticulina discipiens* Wisniewski, 1890, bed 40, *Lenticulina muensteri* Assemblage, middle Callovian. **W** *Palmula deslongchampsii* (Terquem, 1864), bed 6, *Protomarssonella poddari*–*Protomarssonella prekummi* Assemblage, middle Bathonian. **X** *Vaginulinopsis epicharis* Loeblich and Tappan, 1950, bed 9, *Spirillina polygyrata* Sub-assemblage, middle Bathonian. **Y** *Vaginulinopsis* cf. *eritheles* Loeblich and Tappan, 1950, bed 9, *Spirillina polygyrata* Sub-assemblage, middle Bathonian. **Z** *Vaginulinopsis* sp., bed 9, *Spirillina polygyrata* Sub-assemblage, middle Bathonian. **AA** *Citharina heteropleura* Terquem, 1868), bed 9, *Spirillina polygyrata* Sub-assemblage, middle Bathonian. **AB** *Reinholdella* sp. bed 22, *Protomarssonella prekummi* Sub-assemblage, lower Callovian



The sample-species occurrence matrix was converted into percentage abundance and then was used for all quantitative analyses (data used in the present study is provided in the Appendix). To identify benthic foraminifera assemblages, the UPGMA (Unweighted Pair Group Method with Arithmetic Mean) clustering was applied using the Bray–Curtis similarity coefficient, which is considered the most suitable measure for abundance data analysis (Clarke and Warwick 2001). The Cophenetic Correlation Coefficient associated with the Bray–Curtis similarity coefficient was the highest relative to other similarity measures (see also Abdelhady and Elewa 2010; Abdelhady and Fürsich 2015). These assemblages were also statistically significant from each other. The Sequential Bonferroni correction was used to govern significant differences at p level = 0.001. Then, the Non-Metric Multidimensional Scaling (NMDS) based on Bray–Curtis similarity was used to visualize these differences. The goodness of fit for the NMDS was assessed by its stress value

(see Abdelhady et al. 2019a, b). Additionally, Canonical Correspondence Analysis (CCA) was performed to rank the importance of the biotic/abiotic factors in shaping the distribution patterns of benthic foraminifera. This method extracts synthetic environmental gradients from ecological datasets (Ter Braak and Verdonschot 1995).

For each sample, biotic (species diversity: Shannon Index, Evenness, and Dominance; shell composition, percentages of agglutinated and calcareous species) and abiotic (BFOI, proxy for oxygen availability; % infauna, a proxy for nutrient availability, sea level, and substrate type) factors were statistically analyzed. The benthic foraminifera taxa, following the categorization of Corliss (1985), Corliss and Emerson (1990) and Corliss and Fois (1990) are separated into three microhabitats: epifaunal (< 1 cm), shallow infaunal (1–4 cm) and deep infaunal (> 4 cm; Corliss 1985, 1991;

Corliss and Emerson 1990; Corliss and Fois 1990). Nutrient and oxygen availability were inferred indirectly through the percentage of infaunal benthic foraminiferal forms (see Van der Zwann et al. 1999; Jain and Collins 2007; Reolid et al. 2008a, b; Garg and Jain 2012; Jain et al. 2019) and by using the Benthic Foraminiferal Oxygen Index (BFOI) of Kaiho (1991, 1994) to infer oxygenation of bottom waters. This index is based on the categorization of benthic foraminifers into three groups, Oxidic (O), Suboxic (S) and Dysoxic (D) based on findings by various authors (see Table 2); BFOI is defined as $[O/(O+D) \times 100]$, where O is the number of oxidic species and D the number of dysoxic species. When $O=0$ and $D+S>0$ (S is the number of suboxic indicators), then the BFOI value is given by $[(S/(S+D)-1) \times 100]$. It must be kept in mind that the BFOI values are only used here to

provide an estimate of the oxygenation of bottom waters as Kaiho (1991, 1994) used modern foraminifera for his analyses as opposed to the Jurassic ones, which are likely to have had a different habitat preference. All data related to species categorization based on their preference for nutrient (trophic group) and oxygen availability (Oxic, O and Dysoxic, D groups for calculating BFOI) along with shell composition (Calcareous and Agglutinated) is provided in Table 3. All statistical analyses were carried out using the PAST V. 2.17 (Hammer et al. 2001) software.

The opportunistic taxa include *Lenticulina*, *Epistomina* and *Eoguttulina*; their increased abundance is suggestive of unstable and deteriorating bottom water conditions (i.e., low oxygen and/or excess nutrients; Reolid et al. 2012; Rita et al. 2016). Shannon index (H), Evenness and

Table 2 Categorization of species based on their life style and shell composition. 1: Tyszka (1995); 2: Olóriz et al. (2003); 3: Nagy et al. (1995); 4: Nagy et al. (2009); 5: Reolid et al. (2012); 6: Rita et al. (2016); 7: Reolid et al. (2008a); 8: Rita et al. (2016); 9: Wasim et al. (2020); 10: This study; 11: Bak et al. (1997); 12: Reolid et al. (2015); 13: Setoyama et al. (2011)

Species	Life style	Shell composition	References
<i>Ammobaculites</i>	Shallow infaunal	Agglutinated	1, 2, 3, 4, 5, 6
<i>Ammodiscus</i>	Epifaunal (phytal)	Agglutinated	7
<i>Astacolus</i>	Shallow infaunal	Calcareous	1, 7, 8
<i>Citharina</i>	Shallow infaunal	Calcareous	5, 9
<i>Citharinella</i>	Shallow infaunal	Calcareous	10
<i>Dentalina</i>	Shallow infaunal	Calcareous	5, 8
<i>Eoguttulina</i>	Shallow to deep infaunal	Calcareous	5
<i>Epistomina</i>	Epifaunal	Calcareous	7, 5
<i>Haplophragmium</i>	Shallow infaunal	Agglutinated	9
<i>Haplophragmoides aeque</i>	Epifaunal	Agglutinated	7
<i>Lenticulina</i>	Deep infaunal	Calcareous	6, 7
<i>Lingulina</i>	Shallow infaunal	Calcareous	5
<i>Marginulina</i>	Shallow infaunal	Calcareous	8, 9
<i>Nodosaria</i>	Shallow infaunal	Calcareous	6, 7
<i>Nubeculinella</i>	Epifaunal/shallow infaunal	Calcareous	7
<i>Ophthalmidium</i>	Epifaunal	Calcareous	7, 8
<i>Palmula</i>	Shallow infaunal	Calcareous	10
<i>Patellina</i>	Epifaunal/shallow infaunal	Calcareous	10
<i>Praedorothia</i>	Shallow to deep infaunal	Agglutinated	11, 12
<i>Proteonina</i>	Shallow infaunal	Agglutinated	9
<i>Protomarssonella</i>	Deep infaunal	Agglutinated	13
<i>Pyramidina</i>	Epifaunal	Calcareous	7
<i>Quinqueloculina</i>	Epifaunal	Calcareous	7
<i>Ramulina</i>	Shallow infaunal	Calcareous	10
<i>Reinholdella</i>	Epifaunal	Calcareous	8
<i>Reophax</i>	Deep infaunal (potentially)	Agglutinated	8
<i>Saracenaria</i>	Shallow infaunal	Calcareous	5, 9
<i>Spirillina</i>	Epifaunal	Calcareous	7, 8
<i>Textularia</i>	Deep infaunal (potentially)	Agglutinated	8
<i>Triloculina</i>	Epifaunal	Agglutinated	7
<i>Tristix</i>	Shallow infaunal	Calcareous	8
<i>Trocholina</i>	Epifaunal	Calcareous	7
<i>Vaginulina</i>	Shallow infaunal	Calcareous	5
<i>Vaginulinopsis</i>	Shallow infaunal	Calcareous	9

humid and arid seasons, whereas lower smectite/kaolinite ratios are suggestive of low sea levels (Chamley 1989, 1997; Deconinck 1992). Additionally, higher smectite (inherited from soils and exported to the open ocean during high sea levels), is suggestive of the presence of extended low relief land areas with a relatively hot climate and seasonal changes in humidity (Chamley 1989). In general, both chlorite and kaolinite are deposited close to shorelines, whereas smectite is transported away from the shore (Adatte and Rumley 1989).

Additionally, based on field and lithological observations (the distribution of lithology—marl, clay, silt, sand and gravel; see also Fürsich et al. 2005, 2014; Roy et al. 2007), coupled with the aforementioned biotic and abiotic parameters, a relative sea level curve was constructed

(Fig. 2). Furthermore, data on the occurrences of shell beds, bored concretions and bioturbation were also integrated within this framework of improved stratigraphy, marked by well-calibrated age-diagnostic ammonites (see also Roy et al. 2007) (Fig. 2). The bathymetric zonation used here is after Olson and Leckie (2003): inner neritic (0–50 m depth), middle neritic (50–100 m depth), outer neritic (100–150 m depth) and upper bathyal (> 150 m depth). The distribution of dominant species and genera (respectively) that account for 80% (trophic nucleus; Rhoads et al. 1972; Oschmann 1991; Reolid et al. 2008b) of the total benthic foraminiferal assemblage is provided in Fig. 4, along with other inferred proxies (% infauna, % opportunistic taxa; % agglutinated taxa; species diversity: Shannon, Evenness, Dominance and Benthic Foraminifera Oxygen Index, BFOI).

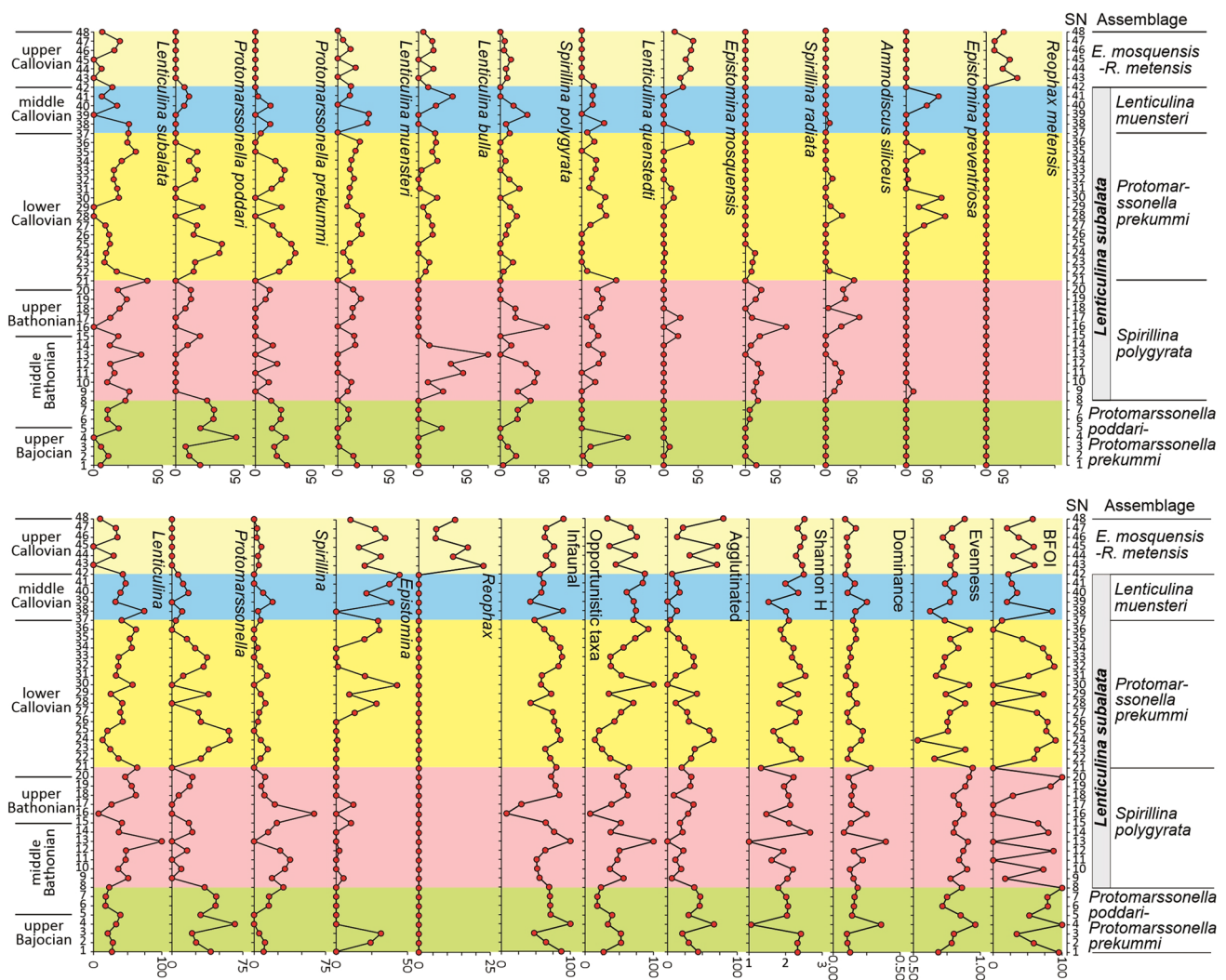


Fig. 4 Distribution of dominant species and genera, and assemblages. **A** Distribution of dominant species. These make up 80% of the total benthic foraminiferal assemblage. **B** Distribution of dominant genera inferred proxies and assemblages. The genus *Lenticulina*, *Protomarrssonella*, *Spirillina*, *Epistomina* and *Reophax* make up 80% of the

total benthic foraminiferal assemblage. The inferred proxies include Infaunal taxa, Opportunistic taxa, Agglutinated, Species diversity indices (Shannon Index, and Dominance) and Evenness, and Benthic Foraminifera Oxygen Index (BFOI). See text for further explanation

Results

Despite the adequacy of samples and species per sample of the present work, there is still an inherent drawback, in the somewhat irregular distribution of samples along the analyzed stratigraphic interval, with adequate samples in certain intervals but a total lack of them in other ones (Fig. 2). The irregular distribution of samples (largely in the uppermost lower Callovian; Formosus and Opis zones) is due to barren samples. A similar barren interval from coeval strata has also been noted by previous workers (Bhalla and Talib 1985a, b, 1991; Bhalla et al. 1998a, b; Talib et al. 2007). Therefore, foraminifera-barren intervals may indicate environmental stress rather than post-depositional diagenetic effects (Schafer et al. 1991). Additionally, the uppermost lower Callovian (Formosus and Opis zones) are monotonous marly silt (Formosus Zone) and sand (Opis Zone) that do not show any taphonomic or sedimentologic biases (see Alhussein 2010, 2014) or biostratigraphic hiatus (ammonites; Roy et al. 2007). The benthic foraminiferal assemblages under study, are thus, considered autochthonous. Additionally, moderate-to-good preservation of benthic foraminiferal species suggests that preservation (with no significant signs of recrystallization, dissolution, or fragmentation) did not greatly alter the primary signal (Fig. 3).

Distribution of dominant species and genera

In general, the upper Bajocian is dominated by *Protomarssonella poddari* and *P. prekummi*, and from the middle Bathonian to the middle Callovian by *Lenticulina subalata*, with secondary dominant species of *Spirillina polygyrata* in the middle Bathonian, *Lenticulina quenstedti* in the upper Bathonian, *L. muensteri* in the lower Callovian, followed by the dominance of *Epistomina mosquensis* and *Reophax metensis* within the upper Callovian (Fig. 4; Table 3).

Five genera (*Lenticulina*, *Protomarssonella*, *Spirillina*, *Epistomina* and *Reophax*) make up 80% of the total benthic foraminiferal assemblage (Fig. 4; Table 3). *Lenticulina* (average value: 38%) has a more or less uniform distribution throughout the section but with relatively lower and fluctuating values in the upper Callovian; *L. subalata* is the most abundant (average value: 14%) and dominates from the middle Bathonian to the middle Callovian (Fig. 4). Subordinate (2nd most dominant taxa) to *L. subalata* for the middle Bathonian to middle Callovian duration include *Lenticulina quenstedti* in the upper Bathonian, *L. muensteri* in the lower Callovian and *L. bulla* in the middle Callovian (Fig. 4). *Protomarssonella*

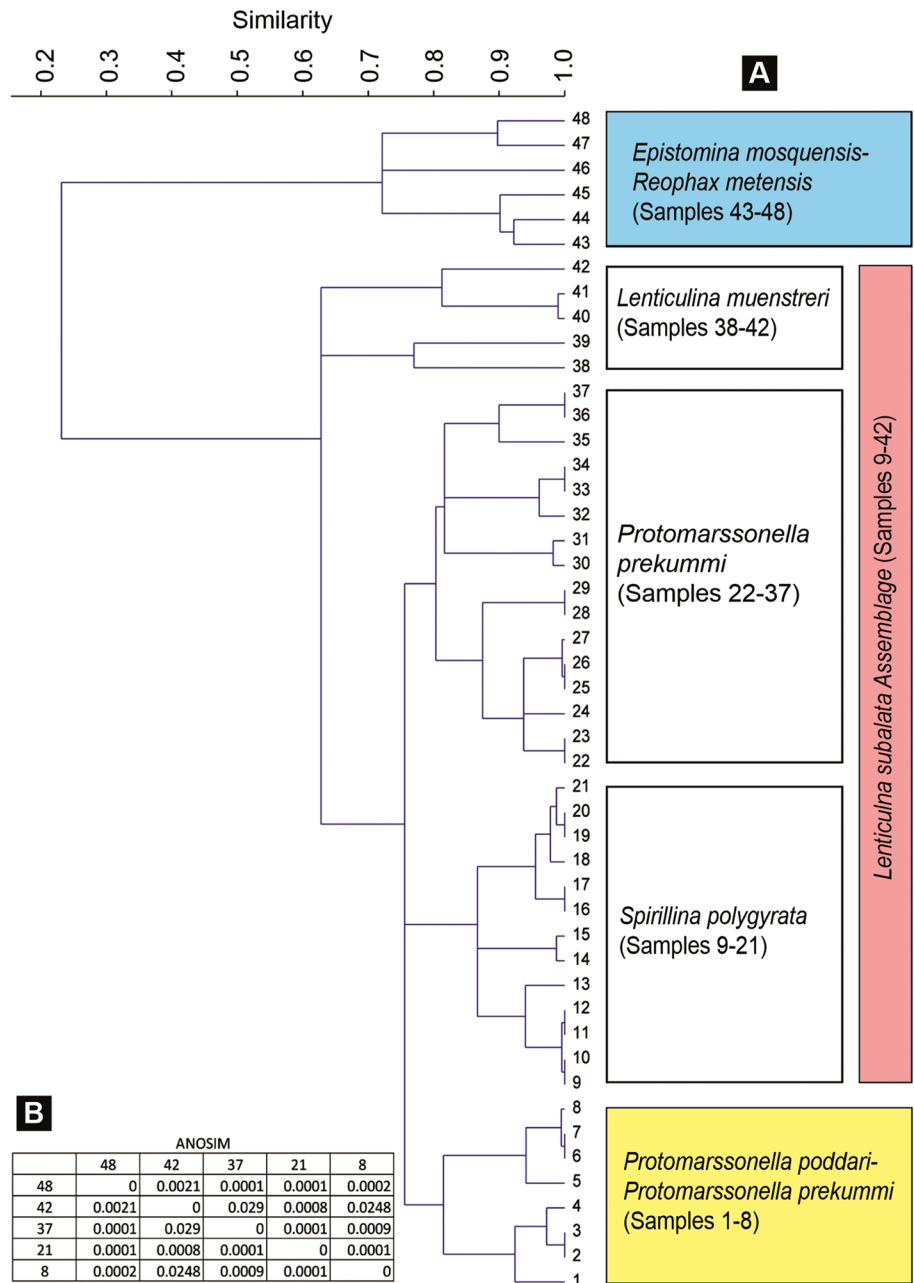
dominates the upper Bajocian to mid-Middle Bathonian interval (samples 1–8; Fig. 4) and makes up 18% of the total benthic foraminiferal assemblage (9% each for *P. poddari* and *P. prekummi*) (Fig. 4). *Spirillina* is largely restricted to the Bathonian and makes up 10% of the total benthic foraminiferal assemblage (7% *S. polygyrata* and 3% *S. radiata*) (Fig. 4). *S. polygyrata* occurs sporadically throughout the section, but it is always a minor fraction (Fig. 4). *Epistomina* (largely *E. mosquensis*) dominates in the upper Callovian (Fig. 4) and makes up 11% of the total benthic foraminiferal assemblage (4% *E. mosquensis*, and 3% *E. preventriosa*) (Fig. 4). *Reophax* (represented only by *R. metensis*) is exclusive to the upper Callovian interval, and forms only a minor fraction (2%) of the total benthic foraminiferal assemblage (Fig. 4).

Of interest is the presence of other agglutinated taxa, besides *Reophax*; that form a sizable fraction throughout the studied section, except during the upper part of lower Callovian to the middle Callovian (= *Lenticulina muensteri* assemblage; see below for assemblage details) (Fig. 4; Table 3). The agglutinated foraminifera form, *Protomarssonella poddari*-*Protomarssonella prekummi* assemblage (upper Bajocian to mid-middle Bathonian) and *P. prekummi* (mid-lower Callovian) sub-assemblage and part of the upper Callovian *Epistomina mosquensis*-*Reophax metensis* assemblage (upper Callovian); *R. metensis* is exclusively restricted to this assemblage (Fig. 4). Both *P. poddari* and *P. prekummi* form ~91% of the total agglutinated assemblage; *R. metensis* makes an additional 6%. Exclusive to the upper Callovian (samples 43–48) and forming 90% (range 77–100%) of the average agglutinated assemblage are: *Ammobaculites* (average % = 18; range: 21 to 31%), *Haplophragmoides* (average % = 22; range 9–73%), *Reophax metensis* (average % = 33; range 16–43%) and *Haplophragmium* (average % = 19; range 14–29%).

Assemblages

To test the relationship among the studied samples, based on their abundance, the Raup-Crick similarity coefficient (CCC = 0.70) was applied that yielded significant differences between assemblages (Fig. 5). Three assemblages are defined by the dominance of *Protomarssonella poddari*-*Protomarssonella prekummi* (samples 1–8), *Lenticulina subalata* (samples 9–42) and *Epistomina mosquensis*-*Reophax metensis* (samples 43–48) (Fig. 5). The *L. subalata* Assemblage (samples 9–42) has three statistically distinct sub-assemblages; these are *Spirillina polygyrata* (samples 9–21), *Protomarssonella prekummi* (samples 22–37) and *Lenticulina muensteri* (samples 38–42; Fig. 5). The percentage abundance of species for the all the assemblages is provided in Table 4.

Fig. 5 Quantitative analyses. **A** UPPGMA clustering (Unweighted Pair Group Method with Arithmetic Mean) dendrogram using the Bray–Curtis similarity coefficient and showing the recognized assemblages and sub-assemblages. **B** Analysis of similarity (ANOSIM) showing the similarities among the recognized assemblages. See text for further explanation. Based on UPGMA clustering (Unweighted Pair Group Method with Arithmetic Mean), three assemblages were identified—*Protomarssonella poddari*–*Protomarssonella prekummi*, *Lenticulina subalata* and *Epistomina mosquensis*–*Reophax metensis*. The *L. subalata* Assemblage has three statistically distinct sub-assemblages; these are (from base to top) *Spirillina polygyrata*, *Protomarssonella prekummi* and *Lenticulina muensteri*



***Protomarssonella poddari*–*Protomarssonella prekummi* assemblage (upper Bajocian to mid-middle Bathonian)**

This assemblage is marked by the dominance of the agglutinated deep infaunal *P. poddari* and *P. prekummi* (Nagy et al. 2009); both make up ~ 38% of the total assemblage (Fig. 5; Table 4). The other major fraction of the assemblage is *Lenticulina* (~ 21%) and *Spirillina* (~ 12%; Table 4). *Lenticulina* is an opportunist with a habitat preference ranging from epifaunal to potentially deep infaunal (Tyszka 1994a, b; Reolid et al. 2008a, b; Reolid et al. 2012; Colpaert et al. 2016; Jain et al. 2019;

Farouk et al. 2020). Both *Spirillina* and *Epistomina* (6.5%; Table 4) are epifaunal (Tyszka 1995, Bouhamdi 2000; Bouhamdi 2001; Olóriz et al. 2003, 2006; Reolid et al. 2008b; Farahani et al. 2018). *Epistomina* is also an opportunist, whereas *Spirillina* is a specialist (Reolid and Martínez 2012; Olóriz et al. 2012; Colpaert et al. 2016). The average % abundance of opportunistic taxa (*Lenticulina* + *Epistomina* + *Eoguttulina*) remains moderately low (averaging 33%) (see also Fig. 4). Substrate-wise, silty clays dominate (samples 1–5) over marly silts (samples 6–8) and the smectite/kaolinite ratio remains low throughout the assemblage (Fig. 2). The BFOI values are

Table 4 Dominant species in the identified assemblages and their percentage abundance

<i>Dorothia poddari-Dorothia prekummi</i>					
Samples 1–8					(%)
<i>Protomarssonella poddari</i>					21.11
<i>Protomarssonella prekummi</i>					16.72
<i>Lenticulina subalata</i>					10.87
<i>Spirillina polygyrata</i>					8.74
<i>Lenticulina muensteri</i>					5.53
<i>Lenticulina quenstedti</i>					4.39
<i>Epistomina khawdensis</i>					3.53
<i>Spirillina radiata</i>					3.22
<i>Epistomina alveolata</i>					2.97
<i>Ophthalmidium carinatum</i>					2.90
Total percentage					80.00
<i>Lenticulina subalata</i>					
<i>Spirillina polygyrata</i>		<i>Dorothia prekummi</i>		<i>Lenticulina muensteri</i>	
Samples 9–21	(%)	Samples 22–37	(%)	Samples 38–42	(%)
<i>Lenticulina subalata</i>	18.02	<i>Lenticulina subalata</i>	14.24	<i>Lenticulina subalata</i>	13.29
<i>Spirillina polygyrata</i>	11.42	<i>Protomarssonella prekummi</i>	14.17	<i>Lenticulina muensteri</i>	12.06
<i>Lenticulina bulla</i>	10.88	<i>Protomarssonella poddari</i>	12.72	<i>Lenticulina bulla</i>	8.98
<i>Lenticulina quenstedti</i>	9.95	<i>Lenticulina muensteri</i>	10.33	<i>Lenticulina quenstedti</i>	8.65
<i>Ammodiscus siliceus</i>	8.91	<i>Lenticulina bulla</i>	6.54	<i>Epistomina preventriosa</i>	7.63
<i>Spirillina radiata</i>	8.06	<i>Lenticulina quenstedti</i>	6.31	<i>Epistomina regularis</i>	7.51
<i>Lenticulina muensteri</i>	7.03	<i>Epistomina preventriosa</i>	5.09	<i>Spirillina polygyrata</i>	5.79
<i>Protomarssonella prekummi</i>	4.47	<i>Spirillina polygyrata</i>	4.44	<i>Epistomina majungaensis</i>	5.01
<i>Protomarssonella poddari</i>	4.35	<i>Quinqueloculina</i> sp.	3.76	<i>Protomarssonella prekummi</i>	4.95
		<i>Triloculina</i> sp.	3.65	<i>Protomarssonella poddari</i>	4.72
		<i>Epistomina mosquensis</i>	3.22	<i>Epistomina mosquensis</i>	3.22
Total percentage	83.10	Total percentage	84.50	Total percentage	81.80
<i>Epistomina mosquensis-Reophax metensis</i>					
Samples 43–48					(%)
<i>Epistomina mosquensis</i>					15.60
<i>Reophax metensis</i>					12.58
<i>Haplophragmoides kutchensis</i>					7.56
<i>Lenticulina subalata</i>					7.68
<i>Textularia jurassica</i>					6.60
<i>Lenticulina bulla</i>					5.66
<i>Haplophragmoides aequale</i>					4.76
<i>Epistomina alveolata</i>					4.60
<i>Lenticulina muensteri</i>					4.28
<i>Spirillina polygyrata</i>					3.66
<i>Haplophragmoides</i> cf. <i>rajnathi</i>					3.53
<i>Ammobaculites reophaciformis</i>					3.50
Total percentage					80.01

relatively high (averaging 75%; Fig. 4). Species diversity (Shannon Index), though moderately high (averaging 2) gradually decreases (2.33 at the base to 1.8 at the top), coincident with increased dominance (0.13 at the base to

0.18 at the top) (Fig. 4). Both the percentage abundances of infauna (averaging 72%) and agglutinated taxa (averaging 41%) are relatively high (Fig. 4; Table 4).

***Lenticulina subalata* assemblage (mid-middle Bathonian-middle Callovian)**

The *Lenticulina subalata* (samples 9 to 42) has three sub-assemblages. These are *Lenticulina subalata-Spirillina polygyrata* (samples 9 to 21), *Lenticulina subalata-Protomarssonella prekummi* (samples 22–37) and *Lenticulina subalata-Lenticulina muensteri* (samples 38–42) (Table 4). The major characteristics of these three sub-assemblages are enumerated below (Figs. 3, 4; Table 4).

***Spirillina polygyrata* sub-assemblage (mid-middle Bathonian-early lower Callovian)** This sub-assemblage is marked by the dominance of calcareous epifaunal species of *Spirillina polygyrata*, 11.4% (Reolid et al. 2008a, b; Jain et al. 2019) and *Spirillina radiata* (8%); *Spirillina* makes up ~20% of the total assemblage (Table 4). The other major fraction of the assemblage is *Lenticulina* (~46%; including *L. subalata*, 18%); both *P. poddari* (4.5%) and *P. prekummi* (4.5%) now only form subordinate fractions (Table 4). The average % abundance of opportunistic taxa is moderately high (averaging 50%) (Fig. 4). Substrate-wise, marly silts are noted except for clays in samples 13 to 15 (Fig. 2). The smectite/kaolinite ratio is the highest for the studied section (Fig. 2). The BFOI values are moderate (averaging 41%; see Fig. 4). Species diversity (Shannon Index), is moderate (averaging 1.9); it gradually reduces (2 at the base to 1.3 at the top) coincident with increased dominance (0.15 at the base to 0.28 at the top) (see Fig. 4). The percentage abundance of infauna taxa remains high (averaging 63%), but that of the agglutinated taxa is low (averaging 20%; Fig. 4).

***Protomarssonella prekummi* sub-assemblage (mid-lower Callovian)** This sub-assemblage is marked by the dominance of agglutinated deep infaunal (Setoyama et al. 2011) species of *Protomarssonella poddari* and *P. prekummi*; both make up ~27% of the total assemblage (Table 4). The other major fraction of the assemblage is *Lenticulina* (~37%; including *L. subalata*, 14%) and *Epistomina* (~8%; *E. preventriosa*, 5%, *E. mosquensis*, 3.2% (Table 4). *Epistomina* is an opportunist with a shallow infaunal habitat (Reolid et al. 2013; Jain et al. 2019). The average % abundance of opportunistic taxa is moderately high (averaging 51%). Substrate-wise, marly silts prevail. The smectite/kaolinite ratio remains high, but gradually reduces up section (Fig. 2). The BFOI values are moderate (averaging 53%); they reduce gradually up section, from an assemblage high of 60 at the base to a low of 13, at the top (Fig. 4). Species diversity (Shannon), remains moderately high (averaging 2.13) and species dominance gradually increases (0.11 at the base to 0.15 at the top; Fig. 4). Both the percentage abundances of infauna (averaging 70%) and agglutinated taxa (averaging 28%) are relatively high (Fig. 4).

***Lenticulina muensteri* sub-assemblage (upper lower Callovian to middle Callovian)** This sub-assemblage is marked by the dominance of *Lenticulina* (~50%; including *Lenticulina subalata*, ~13%) and *Epistomina* (~23%) (Table 2). *Lenticulina*, *Epistomina*, *Spirillina* and *Protomarssonella* make up 89% of the total assemblage. The average % abundance of opportunistic taxa is high (averaging 76%). Substrate-wise, silts dominate over silty clays (Table 4). The smectite/kaolinite ratio remains very low (Fig. 2). The BFOI values are low (averaging 38%); they reduce gradually up section, from an assemblage high of 86% at the base to a low of 22%, at the top (Fig. 4; Table 4). Species diversity (Shannon Index) remains moderately high (averaging 2.08) and increases up section, from an assemblage low of 2 at the base to a high of 2.5, at the top (Fig. 4). Species dominance gradually reduces (0.25 at the base to 0.09 at the top; Fig. 4). The percentage abundance of the infauna taxa (averaging 61%) reduces from an assemblage high of 89% at the base to a low (56%) at the top (Fig. 4). The percentage abundance of agglutinated taxa (averaging 10%) is low and reduces from an assemblage high of 14% at the base to a low of 7%, at the top (Fig. 4).

***Epistomina mosquensis-Reophax metensis* assemblage (upper Callovian)**

This assemblage is marked by the dominance of *Epistomina* (~20%), *Lenticulina* (~17%; including *Lenticulina subalata*, ~7%), and the agglutinated taxa of *Reophax* (*R. metensis*; 12.5%) and *Haplophragmoides* (~16%; Fig. 4; Table 4). The agglutinated forms show an overall dominance within this assemblage, making up ~38% of the total assemblage (Table 4). The average % abundance of opportunistic taxa is moderately high (averaging 55%). Substrate-wise, silty clays prevail (Table 4); the smectite/kaolinite ratio remains low (Fig. 2). The BFOI values are low (averaging 44%; Fig. 4). Species diversity remains relatively high (averaging 2.4) and increases up section, from an assemblage low of 2.46 at the base to a high of 2.51, at the top (Fig. 4). Species dominance gradually reduces (0.11 at the base to 0.09 at the top; Fig. 4). The percentage abundance of the Infauna taxa is very high (averaging 72%) and increases from an assemblage low of 75% at the base to a high of 90%, at the top (Fig. 4). The percentage abundance of agglutinated taxa is moderately high (averaging 48%) and increases from an assemblage low of 71% at the base to a high of 80%, at the top (Fig. 4).

Biotic traits

The species diversity (Shannon Index) consistently remains below 2.67 and Dominance remains below 0.30, except for two values of 0.36 (sample 4; upper Bajocian) and 0.39 (sample 13; middle Bathonian; Figs. 4 and 6).

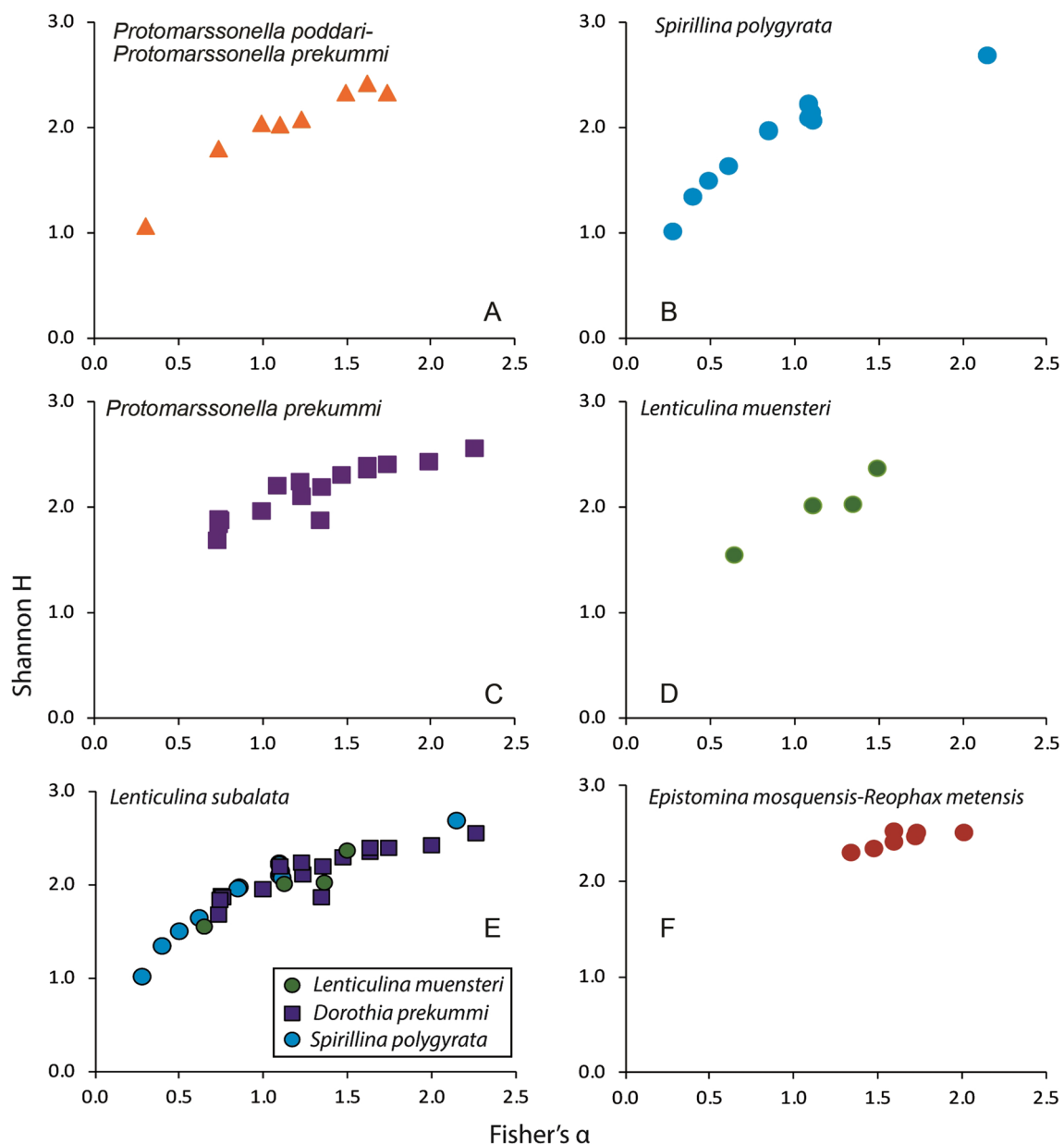


Fig. 6 Community structure and depositional environment of the studied section. The plot of Fisher's α versus Shannon Index gives a robust estimate of the depositional environment and the prevailing foraminiferal community structure. All data points that plot between the values of 5 (Fisher's α) and 2.5 (Shannon Index) belong to the restricted lagoonal region. See text for further explanation. The

illustrated assemblages include: *Protomarssonella poddari*–*Protomarssonella prekummi* (A), *Lenticulina subalata* (E) and *Epistomina mosquensis*–*Reophax metensis* (F). The *L. subalata* Assemblage has three statistically distinct sub-assemblages; these are (from base to top) *Spirillina polygyrata* (B), *Protomarssonella prekummi* (C) and *Lenticulina muensteri* (D)

The plot of Fisher's α versus Shannon Index gives a good idea of the depositional settings (i.e., restricted vs. open marine) of the studied benthic foraminiferal fauna (Murray 1991; Farouk and Jain 2016, 2017; Jain and Farouk 2017). Scatter plots between 5 (Fisher's α) and 2.5 (Shannon Index) are considered to fall within the restricted lagoonal/littoral setting region (see Murray 1991, 2006; Farouk and Jain 2016, 2017; Jain and Farouk 2017). The plot of the Shannon

Index and Fisher's α (Fig. 5) reveals a spread of data within the restricted lagoonal/littoral setting region (Fig. 6).

The percentage abundance of infaunal benthic foraminifera taxa across the section is moderate to high (averaging 70%; between 8 and 100%) with lower values in the upper Bathonian (<70%; Fig. 4; Table 4). The BFOI values are relatively higher, throughout the studied section but with somewhat lower values in upper Bajocian and early lower

Callovian (Fig. 4; Table 4). The % of agglutinated foraminifera makes a sizable fraction in the upper Bathonian, early lower Callovian (samples 16 to 24), and upper Callovian (samples 43 to 48; see Fig. 4).

To find the relationships between the benthic foraminifera and their environmental controls in addition to ranking their influences, the Canonical Correspondence Analysis (CCA) was applied to the occurrence matrix (observation) and the biotic/abiotic traits. The overall quality of the fit is good, where the first four-axes comment on 82.4% of the total variance; axes 1 to 4 explain 38.6%, 19.6%, 15.6% and 8.7% of the data, respectively (see Table 5). Sea level (Axis 1), BFOI (oxygen preference) and % infaunal (paleoproductivity; Axis 2) are the main factors controlling the benthic foraminiferal distribution patterns (Table 5).

Discussion

No strong taphonomic signatures on the shells (recrystallization, dissolution, or fragmentation) were found. The shells also have moderate-to-good preservation and no reworking signature on sediments (monotonous marly silt), and thus, the foraminiferal assemblage considered autochthonous and preserve primary signal. Therefore, they can be used to reconstruct the paleoenvironment.

Bathymetry

The species-based bathymetric data for the Middle Jurassic is very scarce (Murray 1991, 2006; Nagy et al. 2009; Farahani et al. 2018; Jain et al. 2019; Malik et al. 2020). Hence, other proxies such as field observations (substrate type), clay mineralogy (smectite/kaolinite ratio), shell beds, types of concretions (bored/Fe-concretion), diversity plot (Shannon Index versus Fisher's α) and macrofaunal content such as the presence of corals and sponges are incorporated with the

available benthic foraminiferal species- and genera-based inferences, to arrive at the bathymetric estimate.

In terms of bathymetry for the basal agglutinated *Protomarssonella poddari*-*Protomarssonella prekummi* assemblage (upper Bajocian to mid-middle Bathonian; samples 1–8), the presence of shell beds, bored concretions, cross-bedding, the oolitic nature of the limestone beds, and silty clays are suggestive of shallow inner neritic waters (< 50 m); shallow depth is also reflected in the low smectite/kaolinite ratio (Fig. 2). This depth is also corroborated by the scatter plot of Fisher's α versus Shannon Index, where all assemblage data points plot within the restricted lagoonal/littoral settings (Fig. 6A; all points plot between 0 and 1.5 Fisher's α axis) (see also Murray 1991; Hess et al., 2014; Jain and Farouk 2017). The lower siliciclastic samples (1–5; upper Bajocian) are marked by the increased relative abundance of epistominids (*Epistomina khawdensis* and *E. alveolata*; ranging from 24 to 31%; see also Appendix); *Epistomina* has been noted to occur in higher abundances in muddy sea bottoms (Le Galvez 1958; Gradstein 1978; Bernier 1984; Stam 1985; Meyer 2000; Samson 2001; Olóriz et al. 2003) or even in shallow waters in fine-grained sediments such as silty clays (as in the present case) (Bartenstein and Brand 1937; Riegraf 1985; Riegraf and Luterbacher 1989; Tyszkla 1994a, b; Sagasti and Ballent 2002), corroborating shallow waters. However, up section (samples 6–8; middle Bathonian) the presence of marly silts and increasing carbonates is suggestive of a somewhat deeper setting; this is also reflected by the record of an ammonite (Fig. 2; see Roy et al. 2007) and the presence of *Spirillina* (*Spirillina polygyrata* and *S. radiata*) (see Fig. 4; Table 4). Hence, for the *P. poddari*-*P. prekummi* assemblage, an inner neritic (< 50 m) depth is proposed for samples 1–5, and a depth close to the inner to the middle neritic boundary (50–75 m; samples 6–8).

The *Spirillina polygyrata* sub-assemblage (mid-middle Bathonian to lower Callovian; samples 9–21) is characterized by the highest values of smectite/kaolinite ratio (Fig. 2). Higher values are indicative of warm climates and transgressive seas (Chamley 1989, 1997; Deconinck 1992) (Fig. 2). Additionally, both the GYFM (limestone-marl alternations) and the succeeding Sponge Limestone Member (SLM: limestone-marl alternations) were deposited below the storm-wave base with rare presence of storm-induced currents (Fürsich et al. 2014), and thus, are also suggestive of a deepening TST regime (Fig. 2). Additionally, the presence of sponges (within the SLM) suggests well-oxygenated, clear and warm bottom waters and within the lower part of the photic zone close to a middle-outer neritic depth boundary (Jain et al. 2019). At coeval levels in the neighboring locality, the SLM Member exposed at Jumara (Fig. 1B), Mehl and Fürsich (1997) recorded a rich assemblage of "lithistid" demosponges and dictyonal hexactinellinids with rare calcisponges (calcareous sponges); the sponge meadow

Table 5 Loading of the first four axes of the Canonical Correspondence Analysis (CCA). Paleoproductivity (% infauna) and oxygen preference (Benthic Foraminifera Oxygen Index; BFOI) associated with sea-level changes are considered as major factors controlling the distribution pattern of the benthic foraminifera

Variables	Axis 1	Axis 2	Axis 3	Axis 4
% of variance	38.6	19.6	15.6	8.7
Sea level (m)	0.74	0.08	-0.45	-0.21
Sediment type (Substrate)	-0.52	-0.16	-0.08	-0.24
% Infauna	0.12	-0.82	0.42	-0.16
BFOI	0.18	-0.95	0.07	-0.09
% Calcareous taxa	-0.48	0.68	-0.44	0.15
% Agglutinated taxa	0.48	-0.68	0.44	-0.15
Number of taxa	0.31	-0.32	-0.14	0.30
Shannon H	0.35	-0.25	-0.09	0.30
Species dominance	-0.28	0.18	0.06	-0.29

grew on a carbonate ramp at the lower end of the photic zone, in quiet waters below storm wave base, a position not below mid shelf (i.e., middle neritic) (see also Leinfelder et al. 1993; Olóriz et al. 2003). Mehl and Fürsich (1997) also noted that the sponges from the SLM at Jhura (this study) are suggestive of much shallower depth than those recorded from the Jumara Dome. The benthic foraminifera, *Spirillina polygyrata* also prefers middle neritic depths (Murray 1991, 2006). Relatively, deeper depth is also corroborated by the presence of *Epistomina mosquensis* (relative abundance range: 10–12%, average 1.7%, respectively; see Appendix). *Ophthalmidium strumosum* indicates high nutrients (Reolid and Martínez-Ruiz 2012). The scatter plot of Fisher's α versus Shannon Index is indicative of restricted environmental conditions; all points plot between 0 and 1.5 Fisher's α axis (Fig. 5B). Contextually, the rarity of aragonitic-shelled *E. mosquensis* and of bivalves may also suggest that the fauna might have undergone diagenetic dissolution of the aragonitic elements. However, corals (*Dimorphariaea*, *Montlivaltia*, *Amphiasirea* and *Isastrea*) and bivalves (*Tendagurium* and *Trigonopsis*) that originally possessed aragonitic skeletal material, are recorded as well and in abundance (see Mehl and Fürsich 1997; Fürsich et al. 2014). Additionally, moderate-to-good preservation of benthic foraminifera also suggests that dissolution did not greatly affect the composition of the assemblages, under study (Fig. 3). Hence, for the *Spirillina polygyrata* sub-assemblage, a conservative middle neritic depth (~75 m) is proposed but in a somewhat restricted environmental condition (deeper lagoonal).

The *Protomarssonella prekummi* sub-assemblage (mid-lower Callovian; samples 22–37) is somewhat deeper than the *P. poddari*–*P. prekummi* assemblage due to the presence of epistominids (*Epistomina preventriosa* and *E. mosquensis*; see also Tables 3, 4); *Epistomina* is a characteristic middle to outer neritic form with a preference for marl-clay substrates (Stam 1986; Murray 1991; Olóriz et al. 2012; Reolid et al. 2008a, b). *Spirillina polygyrata* prefers middle neritic depths (Murray 1991). Additionally, the marly slit substrate and the relatively higher smectite/kaolinite ratios are also suggestive of deeper depths; however, the gradual decrease of the ratio up section, suggests some shallowing and increased terrigenous input (Fig. 2; see Alcalá, et al. 2013). Deeper conditions are also noted in the scatter plot of Fisher's α versus Shannon Index, where most points plot higher than the *S. polygyrata* sub-assemblage (Fig. 6B), i.e., between 0.5 and 2.5 Fisher's α axis (Fig. 6C). Species diversity (Shannon) is also the highest with lowest species Dominance for the assemblage, suggestive of deeper equitable conditions (Fig. 4).

The *Lenticulina muensteri* sub-assemblage (upper lower Callovian to middle Callovian; samples 38–42) is marked by the near dominance of *Lenticulina* (~50%; Table 4). Genus *Lenticulina* is a poor bathymetric indicator. Hence,

of bathymetric interest within this assemblage, is the presence of middle neritic depth preferring epistominids (~24%) and *Spirillina* (~6%) in the lower part of the assemblage, and of *Protomarssonella poddari* and *P. prekummi* (~5% each) in the upper part (Fig. 4; Table 3), suggesting shallowing upwards. The increased presence of *Protomarssonella* also coincides with a shift in lithology from marly silt to silt (Fig. 2), suggesting shallowing and increased terrigenous input. Hence, for samples 38–39 (with abundance of *Lenticulina*, *Epistomina* and *Spirillina*; lower Callovian), a middle neritic (75–100 m) depth is suggested, whereas for samples 40–42 (*Lenticulina*, *Epistomina* and *Protomarssonella*; middle Callovian), a somewhat shallower inner to middle neritic boundary depth is suggested (50–75 m). Shallow depth is also corroborated by the lowest smectite/kaolinite ratios and the presence of sandstones with occasional Fe-concretions, up section (Fig. 2). Additionally, of all the three sub-assemblages of the *Lenticulina subalata* assemblage (samples 9–42; Fig. 6E), the *L. muensteri* sub-assemblage (Fig. 6D) represents an intermediate depth position in the scatter plot of Fisher's α versus Shannon Index, straddling between the deeper *Spirillina polygyrata* (Fig. 6B) and the shallower *Protomarssonella prekummi* sub-assemblages (Fig. 6C).

The *Epistomina mosquensis*–*Reophax metensis* assemblage (upper Callovian; samples 43–48) is characterized by the exclusive presence of the agglutinated *Haplophragmoides* (*H. aequale*, range: 4–7% and *H. cf. rajnathi*, 3.6–9.2%), *Ammobaculites* (*A. reophaciformis*, 1.3–7.6%, *A. coprolithiformis*, 3.6–4.7%, *A. fontinensis*, 2.2–4.7% and *A. subcretaceus*, 3.1–6.7%), *Haplophragmium* (*H. kutchensis*, 4–14.3%, and *H. inconstans*, 5.9%) and *Textularia jurassica* (4.3–13%) (Table 3; see also Appendix). The latter four genera are suggestive of inner neritic depths (<50 m), however, the dominance of both *E. mosquensis* (8–23%) and *R. metensis* (6–23%) (Fig. 4), and the high smectite/kaolinite ratios (Fig. 2) suggest somewhat deeper middle neritic depths (75–100 m); both *Reophax* and *Epistomina* (~40% of the total assemblage) prefer middle neritic depth (Stam 1986; Olóriz et al. 2003; Reolid et al. 2008a, 2013). *Reophax* is represented only by *R. metensis*, whereas *Epistomina* is represented by *E. mosquensis* (8–22%), *E. alveolata* (2.1–12%), *E. majungaensis* (7.5%), and *E. regularis* (7.1%); the latter two are restricted to sample 46, only (see Appendix). Nagy and Johansen (1989) noted that *R. metensis* is less common in low diversity arenaceous assemblages reflecting basal delta front environments, and is quite sporadic in high diversity, in dominantly calcareous assemblages of marine shelf conditions (see also Kaminski et al. 1988; Jenkins 2000). A deeper setting is also corroborated by the scatter plot of Fisher's α versus Shannon Index as all data points plot in relatively higher values between 1.25 and 2 Fisher's α axis (Fig. 6F) (see also Murray 1991; Farouk and Jain 2016, 2017; Jain and Farouk 2017). Studies have

demonstrated that in the cross-plot of Fisher's α and Shannon Index, lower values reflect shallow restricted (largely lagoonal/littoral) conditions, whereas higher values are suggestive of deeper open marine settings (see Murray 1991; Farouk and Jain 2016, 2017; Jain and Farouk 2017). Hence, for the *E. mosquensis*–*R. metensis* assemblage, a conservative middle neritic depth (75–100 m) is proposed.

Interestingly, the aforementioned bathymetric control is also corroborated by the results of the quantitative analysis (Canonical Correspondence Analysis, CCA) where sea level is one of the major factors ($r = -0.74$ for the first axis), whereas sediment type (substrate) is the 2nd major factor; $r = -0.52$) controlling the benthic foraminiferal distribution patterns (Table 5). This quantitative multivariate method has enabled us to rank the importance of each parameter that shapes the foraminiferal distribution patterns within the studied section (Palmer 1993; Ter Braak and Verdonschot 1995). A summary of inferred paleodepths for each assemblage and the distribution of the recorded assemblages is provided in Table 6 and Fig. 7.

Of interest is the close correspondence of the Fisher's α versus Shannon Index plot with inferred paleodepths based on characteristic benthic foraminiferal assemblages (Fig. 6). Both the inferred paleodepth (bathymetry, as discussed above) and diversity plot-based estimates suggest *P. poddari*–*P. prekummi* as the shallowest and *E. mosquensis*–*R. metensis* as the deepest assemblage, largely within middle to outer neritic depths (Fig. 6).

Paleoenvironment

In general, all benthic foraminiferal assemblages are associated with ammonites (Fig. 2) suggesting an open marine environment with normal salinity (Fig. 7) (Seidenkrantz 1993; Nagy et al. 1995, 2010a, b; Nagy and Seidenkrantz 2003; Olóriz et al. 2006, 2012; Nagy and Berge 2008). Also, the presence of siliceous sponges in some facies support waters with normal salinity.

The *Protomarssonella poddari*–*P. prekummi* assemblage is marked by the relative abundance of

Protomarssonella (38%), *Lenticulina* (21%), *Spirillina* (12%) and *Epistomina* (6%) (Fig. 4; Table 3). Both *Lenticulina* and *Epistomina* are opportunistic taxa and thus, can thrive in different trophic resource conditions, from low (oligotrophic) to high (eutrophic) nutrient availability (Reolid et al. 2008a). But the presence of epifaunal *Spirillina* that prefers well-oxygenated and mesotrophic waters with low rates of sedimentation (Gaillard 1983; Reolid et al. 2008a, b; Springer et al. 2016; Jain et al. 2019) and that of the shallow infaunal *Protomarssonella* suggests that the environment was mesotrophic (as also reflected by high abundance of infauna, averaging 72%), well-oxygenated (as reflected by high species diversity and high BFOI values). Bouhamdi et al. (2001) based on their study from the middle Oxfordian of southeastern France linked the increased abundance of spirillinids to higher nutrient availability. Thus, for the *P. poddari*–*P. prekummi* assemblage, a well-oxygenated and moderately mesotrophic waters with low rates of sedimentation is suggested (Figs. 7, 8).

The opportunist *L. subalata* is a major component in all three sub-assemblages, hence, the next two dominant species are considered as nominal species for their respective sub-assemblages (see Figs. 4, 5 and 7).

The *Spirillina polygyrata* sub-assemblage (mid-middle Bathonian–lowermost Callovian; samples 9 to 21) is dominated by *Lenticulina* (46% of the total assemblage), *Spirillina* (19%), *Protomarssonella* (9%) and *Ammodiscus* (5%) (Table 4; Appendix). The epifaunal *Spirillina* prefers oxic environments (Rita et al. 2016 and references, therein; see also Table 2). The epifaunal agglutinated *Ammodiscus* (Reolid et al. 2008a) (see Table 2) also suggests oxygenated bottom waters, but the presence of shallow to deep infaunal *Protomarssonella* (Bak et al. 1997; Reolid et al. 2015) associated with relatively lower BFOI values, higher values for % opportunistic and infauna taxa, reduced species diversity (Shannon, averaging 1.9), and increased species dominance (reaching 0.28) are suggestive of moderately oxygenated and moderately mesotrophic conditions (Figs. 7, 8). Probably, oxygen was depleted below the sediment–water interface.

Table 6 Proposed paleodepths inferred for the identified assemblages (in bold) and sub-assemblages noted in the present study

Assemblage/Sub-assemblages	Sample nos	Age	Inferred paleodepth	
<i>Epistomina mosquensis</i> – <i>Reophax metensis</i>	43–48	Upper Callovian	Middle neritic	75–100 m
<i>Lenticulina subalata</i>				
<i>Lenticulina muensteri</i>	38–42	Lower Callovian to middle Callovian	Inner to middle neritic boundary	50–75 m
<i>Protomarssonella prekummi</i>	22–37	Mid-lower Callovian	Middle neritic	75–100 m
<i>Spirillina polygyrata</i>	9–21	Mid-middle Bathonian to lower Callovian	Middle neritic	~75 m
<i>Protomarssonella poddari</i> – <i>Protomarssonella prekummi</i>	1–8	Upper Bajocian to mid-middle Bathonian	Inner to middle neritic boundary	50–75 m

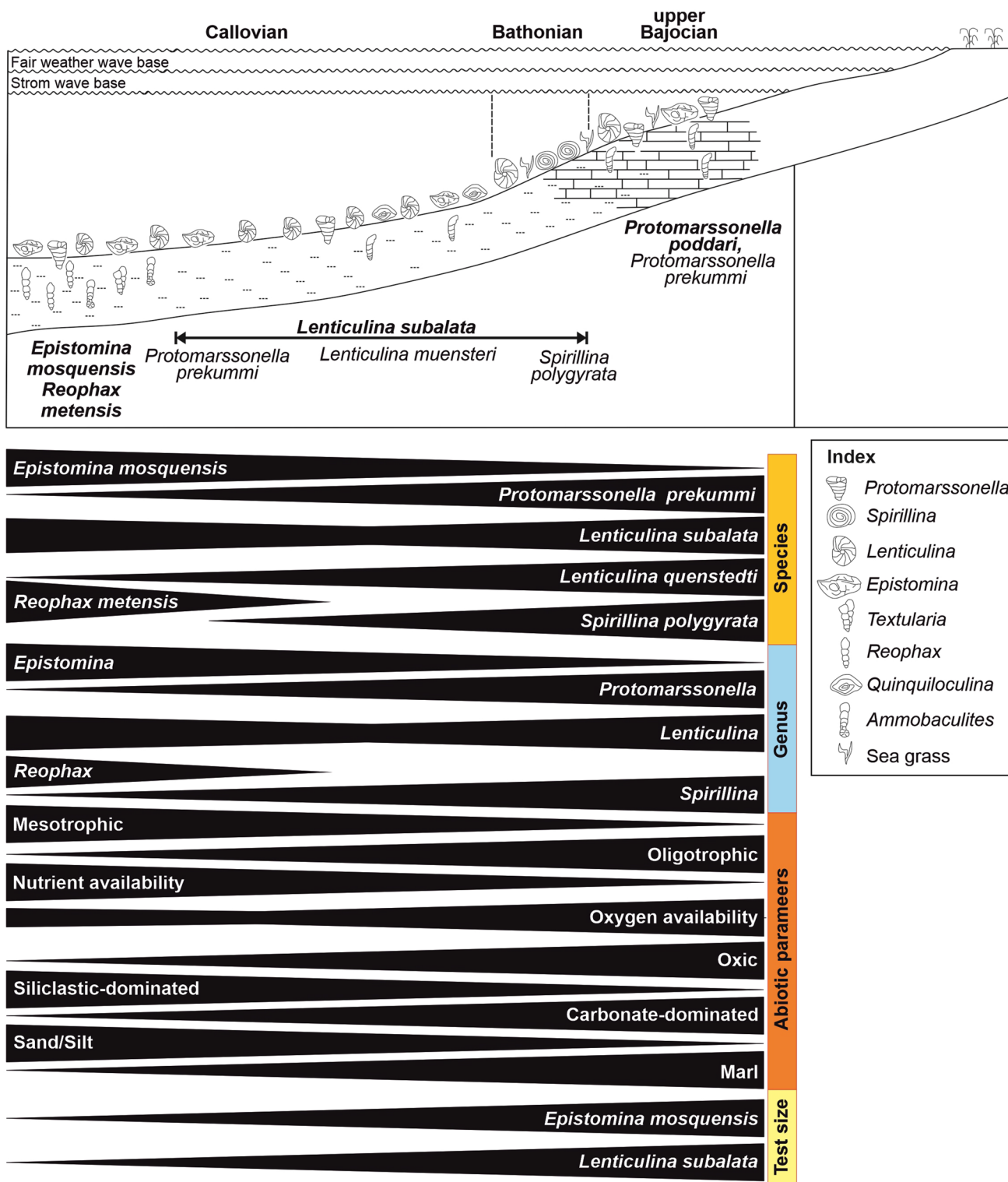


Fig. 7 Bathymetric distribution of foraminiferal taxa and lateral distribution of abiotic and abiotic factors discussed in the text and used in the present study for the Jhura Dome

The *Protomarssonella prekummi* sub-assembly reflects adverse bottom water conditions such as turbidity, as also indicated by the presence of marly silts throughout the

assembly (Fig. 2). A gradually reducing smectite/kaolinite ratio (Fig. 2) is also suggestive of increased shallowing and/or increased temperature and humidity in continental

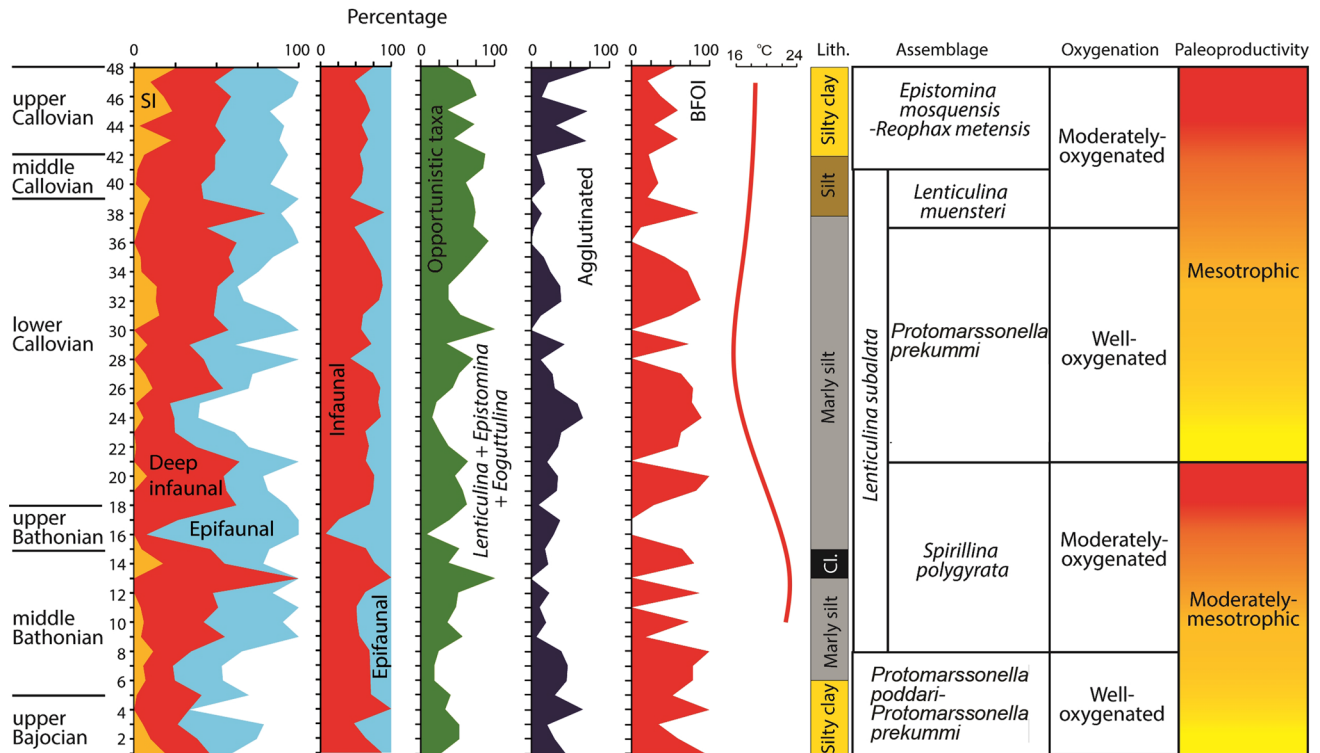


Fig. 8 Inferred paleoenvironment. SN: Sample number; SI: Shallow Infaunal; BFOI: Benthic Foraminifera Oxygen Index; Cl.: Clay. The provided paleotemperature is an average (best fit; after Fürsich et al. 2005)

areas, where continental run off was result in an increased input of siliciclastics (Fig. 2) and a corresponding influx of nutrients, thereby favoring the proliferation of opportunistic species (46%: *Lenticulina* and *Epistomina*), agglutinated forms (averaging 28%) and infaunal species (averaging 70%) (Table 3; Figs. 4 and 7). The gradually decreasing trend of the smectite/kaolinite ratio can be correlated to the $\delta^{18}\text{O}$ curve (a proxy of paleotemperature; see Alberti et al. 2012) suggesting clearly that the Bathonian was warmer than the Callovian. Increased nutrients often result in reduced oxygen availability, however, moderate levels of BFOI values (averaging 53%), higher species diversity values (Shannon Index, averaging 2.13) and low species dominance (averaging 0.14) suggests that despite mesotrophic conditions, the bottom waters were relatively well-oxygenated and equitable conditions prevailed (see Figs. 7, 8).

The *Epistomina mosquensis*–*Reophax metensis* assemblage (upper Callovian; samples 43–48) is dominated by *Epistomina mosquensis* (16%; oxic, epifaunal; Reolid et al. 2008a, 2012), agglutinated *Reophax metensis* (12.5%; dys-oxic; potentially deep infaunal; Rita et al. 2016), agglutinated *Haplophragmoides kutchensis* (7.5%; oxic and shallow to deep infaunal; Reolid et al. 2013), *Lenticulina subalata* (7.3%; opportunistic; Reolid et al. 2012; Rita et al. 2016) and the specialist taxa *Textularia jurassica* (6.6%; agglutinated; dysoxic, shallow to deep infaunal; Rita et al. 2016)

(see Table 3). The assemblage is characterized by consistently high values of % infaunal species (averaging 72%; at places as high as 90%) and lower BFOI values (averaging 44%) suggestive of eutrophic to mesotrophic and poor- to moderately oxygenated bottom water conditions (stressed environment) (see also Table 3). However, high species diversity (Shannon Index; averaging 2.4) and low species dominance (0.11–0.09) do not support a poorly oxygenated bottom environment. Increased terrigenous influx (continental run-off of nutrient) has been noted in Kachchh during late Callovian (see Fürsich et al. 2014; Jain et al. 2019) which possibly led to the increased availability of nutrients resulting in lower available oxygen (Fig. 7). Increased siliciclastics (Fürsich et al. 2005) may have also favored the proliferation of agglutinated forms and specialist taxa such as *Reophax*, *Textularia*, *Haplophragmoides*, *Haplophragmium*, *Proteonina*, *Ammobaculites* and *Spirillina*, noted during this assemblage (see Fig. 4 and Appendix). A similar situation of increased species diversity associated with terrigenous influx has also been noted from the Callovian of Scotland (Nagy et al. 2001). Hence, for this assemblage, a mesotrophic and moderately oxygenated bottom water condition is inferred (see Figs. 7, 8).

Thus, based on the available data, for the *Protomarssonella poddari*–*P. prekummi* Assemblage, a well-oxygenated and moderately mesotrophic environment is

inferred (Fig. 8). For the succeeding *S. polygyrata* sub-assembly, a moderately oxygenated and moderately mesotrophic environment is suggested; mesotrophy increases up section (Fig. 8). For the *P. prekummi* sub-assembly, a well-oxygenated and mesotrophic environment is inferred and for the succeeding *L. muensteri* sub-assembly and *E. mosquensis*–*R. metensis* assembly, a moderately oxygenated and mesotrophic environment is inferred, where mesotrophy increases up section (Fig. 8).

Thus, in general, within the basin, from the basal *P. poddari*–*P. prekummi* sub-assembly to the top *E. mosquensis*–*R. metensis* assembly, there is a gradual reduction in oxygen availability with a corresponding increase in mesotrophy (increased nutrients = terrigenous flux), from a carbonate-dominated to a siliciclastic-dominated substrate, and from fine marls to coarser silts (Figs. 7, 8). Corresponding with this substrate change is also a reduction in test size of both *Epistomina mosquensis* and *Lenticulina muensteri*, with larger sizes in carbonate-dominated settings (see Alhussein 2010) (Fig. 7). Examples of modern foraminifera inhabiting oxygen restricted environments commonly show size decrease as a result of their rapid reproduction in stressed conditions (see Sen Gupta and Machain 1993; Sen Gupta et al. 2003; Rathburn et al. 2018). Although, in the present study, stressed conditions are noted but the gradual rise in opportunistic species through time (see Fig. 8) points toward a deteriorating bottom water condition, most likely as a result of increased (terrigenous flux = increased nutrients and turbidity) coinciding with a change in climate from a drier and warmer Bathonian to a cooler and humid Callovian (see Alberti et al. 2012). Interestingly, as noted in the discussion above, the quantitative Canonical Correspondence Analysis (CCA) also yielded % infauna (= paleoproductivity; proxy for nutrient availability) and BFOI (oxygen preference) as 3rd and 4th major factors (besides sea level and substrate, as discussed above) controlling of the benthic foraminiferal distribution pattern (Table 5).

Basinal changes

Recently, Jain et al. (2019) and Wasim et al. (2021) quantitatively analyzed the benthic foraminiferal assemblages from the deeper (largely outer neritic) carbonate-dominated setting of the Jumara Dome (Fig. 1). The assemblage changes between the deeper Jumara Dome and the marginally placed Jhura Dome (this study) are subtle (Fig. 9). Basin-ward, at both settings, the Bathonian is dominated by the *S. polygyrata* assemblage, the middle Callovian by *L. subalata* and the upper Callovian by *Reophax metensis* (with *Epistomina mosquensis* at Jhura) (see Fig. 9). The only change in assemblage is during the early Callovian; at Jhura it is represented by the *Protomarssonella prekummi* sub-assembly, whereas at the deeper Jumara locality, it is the *E. mosquensis*

assemblage (Fig. 8). This assemblage change also coincides with a change in facies (from carbonate-dominated Bathonian to siliciclastic-dominated one in the Callovian), climate (from the warm and drier Bathonian to a cooler and wetter Callovian; Fürsich et al. 2005) and increased terrigenous input (= nutrient input) (see Fig. 8). It is plausible that the shallow setting of Jhura, coupled with increased siliciclastic input favored the proliferation and the dominance of agglutinated species as compared to in the deeper Jumara (Fig. 9). The gradual sea-level rise trend toward the latest Callovian is correlated to that of Haq (2018) but the deepening in the early Callovian is much prominent in the studied section. The pattern is also similar to that of the nearby Jumara section (Jain et al. 2019), which indicates a minor role of basinal tectonics, as is the case during the Bajocian–Callovian time interval of the Kachchh Basin.

In terms of species, only eight show meaningful changes between the shallower and deeper localities; these eight species make up 61% of the total benthic foraminiferal assemblages for the studied interval (Fig. 9). The species are *Lenticulina subalata* (average value: 14%), *Protomarssonella poddari* (9%), *Protomarssonella prekummi* (9%), *Lenticulina muensteri* (8%), *Spirillina polygyrata* (7%), *Lenticulina bulla* (7%), and *Epistomina mosquensis* (4%), *Ammodiscus siliceus* (3%; Fig. 9). Both *Lenticulina* and *Epistomina* (average value: 33%; 29% and 4% respectively) are opportunists, whereas the others are specialists, suggesting that within the basin, the bottom environment was stable and equitable, thus, favoring both opportunists and specialists. In general, the dominance of opportunists is indicative of adverse conditions vis-à-vis the restriction of trophic resources (see Reolid et al. 2008a; Farahani et al. 2018).

Higher abundances of *Epistomina* have been noted in relatively deep waters (outer neritic), and in muddy sea bottoms (Gradstein 1978; Bernier 1984; Stam 1986; Samson 2001; Olóriz et al. 2003; Jain et al. 2019) which might also explain the higher abundances of *E. mosquensis* at Jumara (see Figs. 6, 7, 8), a relatively deeper site with considerably more siliciclastic input in the Callovian, as compared to that in the Bathonian (Fig. 9). Additionally, epistominids have also been known to be associated with rising sea levels (Samson 2001; Oxford et al. 2002; Olóriz et al. 2003; Colpaert et al. 2016), which might also explain their increased abundance in the Callovian, rather than in the Bathonian (Fig. 9).

The higher abundance of *Spirillina polygyrata* at the deeper site at Jumara (see Fig. 9) could well be due a combination of the following factors: (1) the species preference for well-oxygenated environments where sedimentation rates are low (see Gaillard 1983; Reolid et al. 2008a, b; Springer et al. 2016), as for the Bathonian at Jumara (see also Fürsich et al. 2014), (2) its preference for warmer seawater temperatures (see Gómez et al. 2009), as is the case

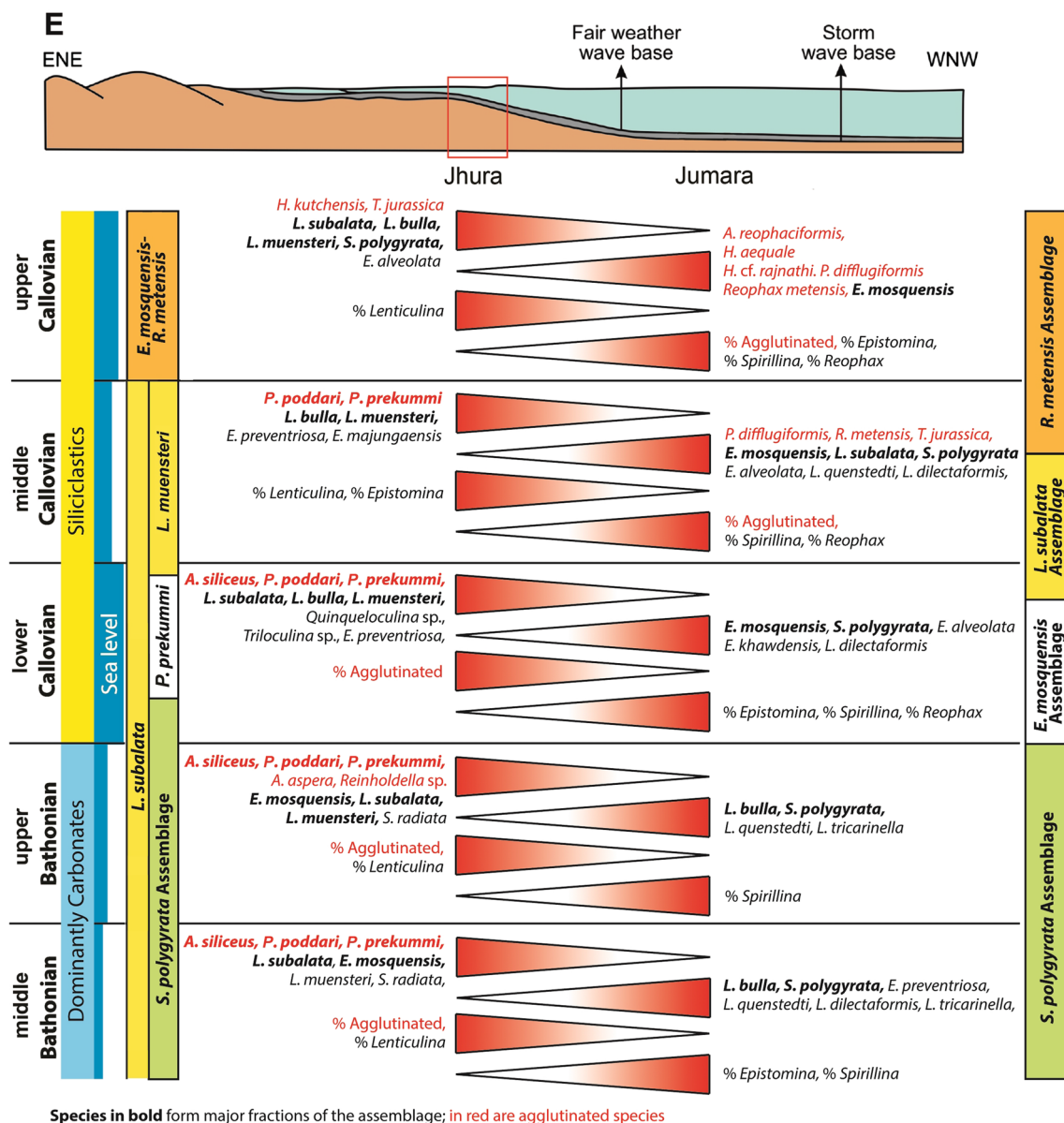


Fig. 9 Bathonian–Callovia assemblage changes between shallower Jhura Dome (this study; inner to middle neritic) and the relatively deeper Jumara Dome (middle to outer neritic; see Jain et al. 2019).

Species in bold form major fractions of the assemblage; in red are agglutinated species. P. = *Protomarssonella*

for the Bathonian carbonates at Jumara (Fürsich et al. 2005), (3) its preference for relatively deeper waters (see Murray 1991; middle neritic depths at Jumara; Jain et al. 2019; early Bathonian maximum flooding horizon in Saudi Arabia; see Kaminski et al. 2020) and, (4) due to substrate type (Stam 1986); its preference for carbonates, as is the case for the Bathonian carbonates at Jumara. Based on the available data (see Figs. 7, 8, 9), it is difficult to differentiate as to which of these played a greater role in defining the abundance of *S. polygyrata*.

The greater abundance of the agglutinated taxa, *Ammodiscus siliceus*, *Protomarssonella poddari* and *P.*

prekummi (Fig. 9) at Jhura is on an expected line, as they prefer shallower depths with greater terrigenous flux (as indicated herein). There is almost no data on *Ammodiscus* and *Protomarssonella* for the Jurassic, hence, for now both substrate type (siliciclastic) and bathymetry could have been responsible for their absence in the deeper upper Callovia interval. Their greater abundance in lower and middle Callovia rocks at Jhura (Fig. 9) coincides with an interval of increased siliciclastic input (Fig. 2).

Conclusions

The analyses of benthic foraminiferal assemblages from the shallow siliciclastic-dominated Jhura Dome (Kachchh basin; Western India) were used to reconstruct the Bajocian to Callovian paleoenvironment. Both biotic (life habit, shell composition, species diversity, and species dominance) and abiotic (sea level and sediment type) parameters were analyzed to determine the main drivers of the benthic foraminifera distribution and abundance. Based on these analyses, we conclude the following:

- Based on UPGMA clustering, three assemblages were identified: *Protomarssonella poddari*–*Protomarssonella prekummi*, *Lenticulina subalata* and *Epistomina mosquensis*–*Reophax metensis*. The *L. subalata* Assemblage has three statistically distinct sub-assemblages; these are (from base to top) *Spirillina polygyrata*, *Protomarssonella prekummi* and *Lenticulina muensteri*.
- Bathymetrically, a paleodepth of inner to middle neritic boundary (50–75 m) is inferred for the *Protomarssonella poddari*–*P. prekummi* assemblage, middle neritic (~ 100 m) for *S. polygyrata* and *P. prekummi* (75–100 m) sub-assemblages, inner to middle neritic boundary (50–75 m) for the *L. muensteri* sub-assemblage and middle neritic (75–100 m) for the topmost *E. mosquensis*–*R. metensis* assemblage.
- In terms of paleoenvironment and based on Canonical Correspondence Analysis (CCA), sea level, substrate type, oxygen preference (BFOI) and paleoproductivity (in order of relevance) are main factors controlling the pattern of benthic foraminiferal distribution.
- For the *Protomarssonella poddari*–*P. prekummi* assemblage, a well-oxygenated and moderately-mesotrophic environment is inferred. For the succeeding *S. polygyrata* sub-assemblage, a moderately oxygenated and moderately mesotrophic environment is suggested; mesotrophy increases up section. For the *P. prekummi* sub-assemblage, a well-oxygenated and mesotrophic environment is inferred and for the succeeding *L. muensteri* sub-assemblage and *E. mosquensis*–*R. metensis* assemblage, a moderately oxygenated and mesotrophic environment, where mesotrophy increases up section.
- In general, within the basin, from the basal *Protomarssonella poddari*–*P. prekummi* to the top *E. mosquensis*–*R. metensis* assemblage, there is a gradual reduction in oxygen availability with a corresponding increase in mesotrophy (increased nutrients = terrigenous flux), from a carbonate-dominated to a siliciclastic-dominated substrate, and from fine marls to coarser silts.
- The benthic foraminiferal species and assemblage changes between the deeper Jumara Dome and the

marginally placed Jhura Dome (this study) are subtle. At both localities, the Bathonian is dominated by the *S. polygyrata* sub-assemblage, middle Callovian by *L. subalata* assemblage and the upper Callovian by *R. metensis* (with *E. mosquensis* at Jhura). The only assemblage change is at the lower Callovian; at Jhura, it is represented by the *Protomarssonella prekummi* assemblage, whereas at the deeper Jumara, it is the *E. mosquensis* assemblage. This assemblage change also coincides with a change in facies (from carbonate- to a siliciclastic-dominated one in the Callovian), climate (from the warm and drier Bathonian to a cooler and wetter Callovian) and increased terrigenous input (= nutrient input) in the Callovian.

- Based on qualitative and quantitative data presented above, it is apparent that the role of nutrients (paleoproductivity) and oxygen availability within a shallow siliciclastic-dominated basin and in a moderately to well-oxygenated bottom water conditions, overrides the influence of bathymetry, that played a far greater role at the deeper setting such as the Jumara Dome than at the shallower Jhura Dome (this study).

Supplementary Information The online version contains supplementary material available at [10.1007/s10347-023-00668-5](https://doi.org/10.1007/s10347-023-00668-5).

Acknowledgements The authors are grateful to two anonymous reviewers for constructive comments and suggestions that greatly improved the manuscript. This work is funded by Researchers Supporting Project number (RSP2023R455), King Saud University, Riyadh, Saudi Arabia.

Data availability All data used in this study was uploaded as online supplementray material (Appendix).

Declarations

Conflict of interest We declare no conflict of interest.

References

- Abdelhady AA, Elewa AMT (2010) Evolution of the Upper Cretaceous oyster. A traditional morphometric approach. In: Elewa AMT (ed) Morphometrics for non morphometricians. Springer Verlag, Cham, pp 157–175
- Abdelhady AA, Fürsich FT (2015) Palaeobiogeography of the Bajocian-Oxfordian macrofauna of Gebel Maghara (North Sinai, Egypt): implications for eustasy and basin topography. *Palaeogeogr Palaeoclimatol Palaeoecol* 417:261–273
- Abdelhady AA, Khalil M, Ismail E, Fan D, Zhang S, Xiao J (2019a) Water chemistry and substrate type as major determinants for molluscan feeding habit and life-mode in lagoon sediments. *Estuar Coast Shelf Sci* 220:120–130
- Abdelhady AA, Khalil M, Ismail E, Mohamed R, Ali A, Snousy M, Fan D, Zhang S, Xiao J (2019b) Potential biodiversity threats associated with the metal pollution in the Nile-Delta ecosystem (Manzala lagoon, Egypt). *Ecol Ind* 98:844–853

- Adatte T, Rumley G (1989) Sedimentology and mineralogy of Valanginian and Hauterivian in the stratotypic region (Jura mountains, Switzerland). In: Wiedmann J (eds) Cretaceous of the Western Tethys Proceedings 3rd International Cretaceous Symposium. Scheizerbart'sche Verlagsbuchhandlung, Stuttgart, pp 329–51
- Alberti M, Fürsich FT, Pandey DK, Ramkumar M (2012) Stable isotope analyses of belemnites from the Kachchh Basin, western India: paleoclimatic implications for the Middle to Late Jurassic transition. *Facies* 58:261–278
- Alcalá FJ, López-Galindo A, Martín-Martín M (2013) Clay mineralogy as a tool for integrated sequence stratigraphic and palaeogeographic reconstructions: late Oligocene–Early Aquitanian western internal South Iberian Margin, Spain. *Geol J* 48(4):363–375
- Alhussein M (2010) Taxonomie und Palökologie der benthischen Foraminiferen aus dem Mitteljura des Kachchh–Beckens, westliches Indien. 160 p., Doctoral Thesis, Würzburg University, Würzburg
- Alhussein M (2014) Taxonomy of the Middle Jurassic benthic foraminifera of the Kachchh Basin, Western India. *Beringeria* 44:51–105
- Bak K, Bak M, Geroch S, Manecki M (1997) Biostratigraphy and paleoenvironmental analysis of benthic foraminifera and radiolarians in Paleogene variegated shales in the Skole unit, Polish Flysch Carpathians. *Ann Soc Geol Pol* 67(2–3):135–154
- Bartenstein H, Brand E (1937) Mikro-paläontologische untersuchungen zur stratigraphie des nordwest-deutschen Lias und Doggers. *Abh Senckenb Naturforsch Ges* 439:1–224
- Bernhard JM (1986) Characteristic assemblages and morphologies from anoxic organic rich deposits: Jurassic through Holocene. *J Foramin Res* 16:207–215
- Bernier P (1984) Les formations carbonatés du Kimméridgien et du Portlandien dans le Jura méridional: documents des Laboratoires de Géologie de Lyon. *Stratigr Micropaléontol Sédimentol* 92:445–803
- Bhalla SN, Talib A (1985a) On the occurrence of foraminifera in the Jurassic rocks of Jhurio hill, central Kutch. *J Palaeontol Soc India* 30:54–56
- Bhalla SN, Talib A (1985) On the occurrence of Foraminifera in the Jurassic rocks of Jhurio Hill Central Kutch. *J Palaeontol Soc India* 30:54–56
- Bhalla SN, Talib A (1991) Callovian-Oxfordian foraminifera from Jhurio hill, Kutch, Western India. *Rev De Paléobiol* 10:85–14
- Bhalla SN, Talib A, Ahmad AHM (1998a) Carbonate microfacies and foraminiferal palaeoecology of Chari Formation (Callovian-Oxfordian), Jhurio Hill, Kutch. *Bull Indian Geol Assoc* 21:17–27
- Bhalla SN, Talib A, Ahmad AHM (1998) Carbonate microfacies and foraminiferal palaeoecology of Chari Formation (Callovian-Oxfordian), Jhurio Hill, Kutch. *Bull Indian Geol Assoc* 31:17–27
- Bouhamdi A (2000) Composition, distribution et évolution des peuplements de foraminifères benthiques de la plate-forme au bassin. Oxfordien moyen du Sud-Est de la France. *Travaux et Documents des Laboratoires de Géologie de Lyon* 151(1): 3–213.
- Bouhamdi AB, Gaillard CH, Ruget CH (2001) Spirillines versus agglutinants: impact du flux organique et intérêt paléoenvironnemental (Oxfordien moyen du Sud-Est de la France). *Geobios* 34(3):266–277
- Canales Fernández ML, García-Baquero G, Henriques MH, Figueiredo VL (2014) Palaeoecological distribution pattern of Early-Middle Jurassic benthic foraminifera in the Lusitanian Basin (Portugal) based on multivariate analysis. *Palaeogeogr Palaeoclimatol Palaeoecol* 410:14–26
- Chamley H (1989) Clay sedimentology. Springer-Verlag, p 623
- Chamley H (1997) Clay mineral sedimentation in the ocean. In: Paquet H, Clauer N (eds) Soils and sediments. Springer-Verlag, Mineralogy and geochemistry, pp 269–302
- Clarke KR, Warwick RM (2001) Change in Marine communities: an approach to statistical analysis and interpretation, 3rd edn. Primer-E Ltd, Plymouth, p 262
- Colpaert C, Nikitenko B, Khafaeva S, Wall AF (2016) The evolution of Late Callovian to Early Kimmeridgian foraminiferal associations from the central part of the Russian Sea (Makar'yev section, Volga River Basin, Russia). *Palaeogeogr Palaeoclimatol Palaeoecol* 451:97–109
- Corliss BH (1985) Microhabitats of benthic foraminifera within deep-sea sediments. *Nature* 314:435–438
- Corliss BH (1991) Morphology and microhabitat preferences of benthic foraminifera from the northwest Atlantic Ocean. *Mar Micropaleontol* 17(3–4):195–236
- Corliss BH, Chen C (1988) Morphotype patterns of Norwegian deep sea benthic foraminifera and ecological implications. *Geology* 16:716–719
- Corliss BH, Emerson S (1990) Distribution of Rose Bengal stained deep-sea benthic foraminifera from the Nova Scotian continental margin and Gulf of Maine. *Deep Sea Research Part A. Oceanographic Research Papers* 37(3): 381–400
- Corliss BH, Fois E (1990) Morphotype analysis of Deep-Sea Benthic Foraminifera from the Northwest Gulf of Mexico. *Palaios* 5(6):589–605
- Deconinck JF (1992) Sedimentologie des argiles dans le Jurassique–Crétacé d'Europe occidentale et du Maroc. *Mémoire d'habilitation à diriger des recherches, Univ Lille*, 249 p
- Enay R, Cariou E (1997) Ammonite faunas and palaeobiogeography of the Himalayan belt during the Jurassic: initiation of a Late Jurassic austral ammonite fauna. *Palaeogeogr Palaeoclimatol Palaeoecol* 134:1–38
- Farahani TS, Reolid M, Yazdia M, Majidifard MR (2018) Benthic foraminiferal assemblages of the Middle and Upper Jurassic sediments from the northeastern Alborz and western Koppeh Dagh, Iran: systematic palaeontology and palaeoecology. *Ann Paléontol* 104:249–265
- Farouk S, Jain S (2016) Benthic foraminiferal response to relative sea-level changes in the Maastrichtian–Danian succession at the Dakhla Oasis, Western Desert, Egypt. *Geol Mag* 155(3):1–18
- Farouk S, Jain S (2017) Sea-level changes in the Paleocene (Danian–Thanetian) succession at the Dakhla Oasis, Western Desert, Egypt: implications from benthic foraminifera. *Proc Geol Assoc* 128:764–778
- Farouk S, Jain S, Belal N, Omran M, Al-Kahtany K (2020) Quantitative Middle Eocene benthic foraminiferal biofacies from west-central Sinai, Egypt: implications to paleobathymetry and sequence stratigraphy. *Mar Micropaleontol* 155:101823
- Fürsich FT (1998) Environmental distribution of trace fossils in the Jurassic of Kachchh (Western India). *Facies* 39:243–272
- Fürsich FT, Pandey DK, Callomon JH, Jaitly AK, Singh IB (2001) Marker beds in the Jurassic of the Kachchh Basin, Western India: their depositional environment and sequence stratigraphic significance. *J Palaeontol Soc India* 46:173–198
- Fürsich FT, Singh IB, Joachimski M, Krumm S, Schlirf M, Schlirf S (2005) Palaeoclimate reconstructions of the Middle Jurassic of Kachchh (western India): an integrated approach based on palaeoecological, oxygen isotopic, and clay mineralogical data. *Palaeogeogr Palaeoclimatol Palaeoecol* 217(3–4):289–309
- Fürsich FT, Pandey DK, Alberti M (2014) Stratigraphy and palaeoenvironments of the Jurassic rocks of Kachchh—Field Guide. *Beringeria, Special Issue 7*, 174 p
- Gaillard C (1983) Les Biohermes à Spongiaires et leur Environnement dans l'Oxfordien du Jura Méridional. *Documents des Laboratoires de Géologie, Université Claude–Bernard, Lyon*, no. 90, 515 p
- Garg R, Jain S (2012) Jurassic Benthic Foraminiferal Diversity, Bathymetry and Paleoenvironment of the Jaisalmer Basin

- (Western India), Neues Jahrbuch für Geologie und Paläontologie – Abhandlungen 263(3): 27–45
- Gaur KN, Singh YP (2000) Foraminiferal composition and biozonation of Callovian–Oxfordian succession, Nara dome, Kutch Mainland, Gujarat, India. *Bull Indian Geol Assoc* 33:43–53
- Gaur KN, Talib A (2009) Middle–Upper Jurassic foraminifera from Jumara Hills, Kutch, India. *Rev Micropaléontol* 52:227–248
- Gebhardt H, Kuhnt W, Holbourn A (2004) Foraminiferal response to sea level change, organic flux and oxygen deficiency in the Cenomanian of the Tarfaya Basin, southern Morocco. *Mar Micropaleontol* 53:133–157
- Gómez JJ, Canales ML, Ureta S, Goy A (2009) Palaeoclimatic and biotic changes during the Aalenian (Middle Jurassic) at the southern Laurasian Seaway (Basque–Cantabrian Basin, northern Spain). *Palaeogeogr Palaeoclimatol Palaeoecol* 275(1):14–27
- Gradstein FM (1978) Jurassic Grand Banks foraminifera. *J Foramin Res* 8:97–109
- Hammer Ø, Harper DAT, Ryan PD (2001) PAST, paleontological statistics software package for education and data analysis. *Palaeontol Electron* 4:1–9
- Haq BU (2018) Jurassic sea-level variations: a reappraisal. *GSA Today* 28(1):4–10
- Jain S (1996) Biostratigraphical and Paleocological Studies of Middle Jurassic (Upper Bathonian–lower Callovian) Beds Exposed in Jumara Dome, Kachchh, Western India. Unpublished Thesis. pp. 202
- Jain S (2014) A new early Middle Bathonian arkelli Chronozone in Kachchh, western India (south Tethys). *Zitteliana* 54:91–146
- Jain S (2019) Middle Bathonian Indonesian *Macrocephalites* cf. *etheridgei* (Spath) from SW Somalia. *J Afr Earth Sc* 151:202–211
- Jain S (2020) The immigration of genus *Macrocephalites* Spath and the Bathonian biostratigraphy of the Kachchh basin (Western India, South Tethys). *Zitteliana* A 94:3–36
- Jain S, Abdelhady AA (2020) Paleobiogeography of the Middle Jurassic (Bathonian–Callovian) benthic foraminifera. *Mar Micropaleontol* 161:101922
- Jain S, Collins LS (2007) Trends in Caribbean paleoproductivity related to the Neogene closure of the central American Seaway. *Mar Micropaleontol* 63:57–74
- Jain S, Farouk S (2017) Shallow Water Agglutinated Foraminiferal response to Late Cretaceous—early Paleocene sea–level changes in the Dakhla Oasis, Western Desert, Egypt. *Cretaceous Research* 78:1–18
- Jain S, Callomon JH, Pandey DK (1996) On the earliest known occurrence of the Middle Jurassic ammonite genus *Reineckeia* in the upper Bathonian of Jumara, Kachchh, Western India. *Paläontol Z* 70:129–143
- Jain S, Collins LS, Hayek LAC (2007) Relationship of benthic foraminiferal diversity to paleoproductivity in the Neogene Caribbean. *Palaeogeogr Palaeoclimatol Palaeoecol* 255:223–245
- Jain S, Abdelhady AA, Alhussein M (2019) Responses of benthic foraminifera to environmental variability: a case from the Middle Jurassic of the Kachchh Basin (Western India). *Mar Micropaleontol*. <https://doi.org/10.1016/j.marmicro.2019.101749>
- Jain S, Niazi M, Abdelhady AA, Vahidinia M, Hossein M (2020) The Campanian paleoenvironment: Inferences based on benthic foraminifera from northeastern Iran. *Palaeogeogr Palaeoclimatol Palaeoecol*. <https://doi.org/10.1016/j.palaeo.2020.109823>
- Jenkins CD (2000) The ecological significance of foraminifera in the Kimmeridgian of Southern England. In: Hart MB, Kaminski MA, Smart CW (eds) *Proceedings of the Fifth International Workshop on Agglutinated Foraminifera*. Grzybowski Foundation Special Publication, 7, pp. 167–178
- Jorissen FJ, De Stigter HC, Widmark JGV (1995) A conceptual model explaining benthic foraminiferal microhabitats. *Mar Micropaleontol* 26:3–15
- Jorissen FJ, Fontanier C, Thomas E (2007) Paleooceanographical proxies based on deep–sea benthic foraminiferal assemblage characteristics. In: Hillaire–Marcel C, de Vernal A (eds) *Proxies in late Cenozoic paleoceanography (part 2)*. Biological tracers and biomarkers. Elsevier, Amsterdam, pp 263–326
- Kaiho K (1991) Global changes of Paleogene aerobic/anaerobic benthic foraminifera and deep–sea circulation. *Palaeogeogr Palaeoclimatol Palaeoecol* 83:65–85
- Kaiho K (1994) Benthic foraminiferal dissolved–oxygen index and dissolved–oxygen levels in the modern ocean. *Geology* 22:719–722
- Kaminski MA (1987) *Cenozoic Deep–Water Agglutinated Foraminifera in the North Atlantic*. Unpublished Thesis. Woods Hole Oceanographic Institution, Woods Bole, MA, USA, 282 p
- Kaminski MA, Setoyama E, Cetaan CG (2008) Revised Stratigraphic Ranges and the Phanerozoic Diversity of Agglutinated Foraminiferal Genera. In: Kaminski MA, Coccioni R (eds) *Proceedings of the seventh international workshop on agglutinated foraminifera*. Grzybowski Foundation Special Publication 13: 79–106
- Kaminski MA, Gradstein FM, Berggren WA, Geroch S, Beckmann JP (1988) Flysch-type agglutinated foraminiferal assemblages from Trinidad: taxonomy, stratigraphy and paleobathymetry. *Abhandlungen Der Geologischen Bundesanstalt* 41:155–227
- Kaminski MA, Setoyama E, Cetaan CG (2010) The Phanerozoic diversity of agglutinated foraminifera: origination and extinction rates. *Acta Palaeontol Pol* 55:529–539
- Kaminski MA, Amao AO, Babalola LO, Balc R, Chan SA, Gull HM, Bu Khamsin A, Malik MH (2020) Benthic foraminiferal assemblages from the Maximum Flooding Surface J30, Middle Jurassic Dhurma Formation, Central Saudi Arabia. *Stratigraphy* 17(4):279–292
- Le Galvez Y (1958) Les foraminifères de la mer Celtique. *Revue Des Travaux De L'institut Des Peches Maritimes* 22:147–194
- Leinfelder RR, Nose M, Schmid DU, Werner W (1993) Microbial crusts of the Late Jurassic: composition, palaeoecological significance and importance in reef construction. *Facies* 29(1):195–229
- Malik MH, Babalola LO, Al-Ramadan K, Kaminski MA (2020) Integrated micropaleontology, sedimentology and sequence stratigraphy of the middle Jurassic D5–D6 Members of the Dhurma Formation, Central Saudi Arabia. *Micropaleontology* 66(6):519–547
- Mehl D, Fürsich FT (1997) Middle Jurassic Porifera from Kachchh, western India. *Paläontol Z* 71(1):19–33
- Meyer M (2000) Le complexe récifal Kimméridgien–Tithonien du Jura meridional interne (France), évolution multifactorielle, stratigraphie et tectonique. 24 179
- Murray JW (1991) *Ecology and palaeoecology of benthic Foraminifera*. Longman Scientific and Technical, Essex, p 397
- Murray JW (2006) *Ecology and applications of benthic Foraminifera*. Cambridge University Press, New York, p 426
- Nagy J (1985) Jurassic foraminiferal facies in the Staffjord area, northern North Sea-i. *J Pet Geol* 8(3):273–295
- Nagy J (1992) Environmental significance of foraminiferal morphogroups in Jurassic North Sea deltas. *Palaeogeogr Palaeoclimatol Palaeoecol* 95:111–134
- Nagy J (2016) A sequence stratigraphic model of benthic foraminiferal facies trends with Triassic and Jurassic examples. *Mar Micropaleontol* 122:99–114
- Nagy J, Berge SH (2008) Micropalaeontological evidence of brackish water conditions during deposition of the Knorringsfjellet Formation, Late Triassic–Early Jurassic, Spitsbergen. *Polar Res* 27:413–427
- Nagy J, Johansen HO (1989) Preservation and distribution pattern *Reophax metensis* (Foraminifera) in the Jurassic of the North Sea. *J Foramin Res* 19:337–348

- Nagy J, Seidenkrantz MS (2003) New foraminiferal taxa and revised biostratigraphy of Jurassic marginal marine deposits on Anholt, Denmark. *Micropaleontology* 49:27–46
- Nagy J, Gradstein FM, Kaminski MA, Holbourn AE (1995) Foraminiferal morphogroups, paleoenvironments and new taxa from Jurassic to cretaceous strata of Thakkhola, Nepal. In: Kaminski MA, Geroch S, Gasinski MA (eds) *Proceedings of the Fourth International Workshop on Agglutinated Foraminifera*. Grzybowski Foundation Special Publication 3, pp. 181–209
- Nagy J, Kaminski MA, Kuhnt W, Bremer MA (2000) Agglutinated foraminifera from neritic to bathyal facies in the Palaeogene of Spitsbergen and the Barents Sea. In: Hart, M.B., Kaminski, M.A., Smart, C.W. (eds) *Proceedings of the Fifth International Workshop on Agglutinated Foraminifera*, vol. 7. Grzybowski Foundation Special Publication, pp. 333–361
- Nagy J, Finstad EK, Dypvik H, Bremer MG (2001) Response of foraminiferal facies to transgressive–regressive cycles in the Caledonian of northeast Scotland. *J Foraminiferal Res* 31(4):324–349
- Nagy J, Reolid M, Rodríguez-Tovar FJ (2009) Foraminiferal morphogroups in dysoxic shelf deposits from the Jurassic of Spitsbergen. *Polar Res* 28:214–221
- Nagy J, Hess S, Alve E (2010a) Environmental significance of foraminiferal assemblages dominated by small-sized *Ammodiscus* and *Trochammina* in Triassic and Jurassic delta-influenced deposits. *Earth Sci Rev* 99:31–49
- Nagy J, Hess S, Alve E (2010b) Environmental significance of foraminiferal assemblages dominated by small-sized *Ammodiscus* and *Trochammina* in Triassic and Jurassic delta-influenced deposits. *Earth Sci Rev* 99(1–2):31–49
- Nagy J, Jargvoll D, Dypvik H, Jochmann M, Riber L (2013) Environmental changes during the Paleocene–Eocene thermal maximum in Spitsbergen as reflected by benthic foraminifera. *Polar Res* 32:19737. <https://doi.org/10.3402/polar.v32i0.19737>
- Olóriz F, Reolid M, Rodríguez-Tovar J (2003) Palaeogeographic and stratigraphic distribution of mid–late Oxfordian foraminiferal assemblages in the Prebetic Zone (Betic Cordillera, Southern Spain). *Geobios* 36:733–747
- Olóriz F, Reolid M, Rodríguez-Tovar FJ (2006) Approaching trophic structure in Late Jurassic neritic shelves: a western Tethys example from southern Iberia. *Earth Sci Rev* 79:101–139
- Olóriz F, Reolid M, Rodríguez-Tovar FJ (2012) Palaeogeography and relative sea-level history forcing eco–sedimentary contexts in Late Jurassic epicontinental shelves (Prebetic Zone, Betic Cordillera): an ecostratigraphic approach. *Earth Sci Rev* 111:154–178
- Olson HC, Leckie RM (2003) Micropaleontological proxies for sea-level change and stratigraphic discontinuities. *SEPM*. <https://doi.org/10.2110/pec.03.75>
- Oschmann W (1991) Distribution, dynamics and palaeoecology of Kimmeridgian (Upper Jurassic) shelf anoxia in western Europe. *Geol Soc Lon Spec Publ* 58(1):381–395
- Oxford MJ, Gregory FJ, Hart MB, Henderson AS, Simmons MD, Watkinson MP (2002) Jurassic planktonic foraminifera from the United Kingdom. *Terra Nova* 14:205–209
- Palmer MW (1993) Putting things in even better order: the advantages of canonical correspondence analysis. *Ecology* 74(8):2215–2230
- Rathburn AE, Willingham J, Ziebis W, Burkett AM, Corliss BH (2018) A new biological proxy for deep-sea paleo-oxygen: pores of epifaunal benthic foraminifera. *Sci Rep* 8:9456. <https://doi.org/10.1038/s41598-018-27793-4>
- Reolid M (2014) Stable isotopes on foraminifera and ostracods for interpreting incidence of the Toarcian Oceanic Anoxic Event in Westernmost Tethys: role of water stagnation and productivity. *Palaeogeogr Palaeoclimatol Palaeoecol* 395:77–91
- Reolid M, Martínez-Ruiz F (2012) Comparison of benthic foraminifera and geochemical proxies in shelf deposits from the Upper Jurassic of the Prebetic (southern Spain). *J Iber Geol* 38:449–465
- Reolid M, Rodríguez-Tovar FJ, Nagy J, Olóriz F (2008a) Benthic foraminiferal morphogroups of middle to outer shelf environments of the Late Jurassic (Prebetic Zone, southern Spain): characterization of biofacies and environmental significance. *Palaeogeogr Palaeoclimatol Palaeoecol* 261:280–299
- Reolid M, Nagy J, Rodríguez-Tovar FJ, Olóriz F (2008b) Foraminiferal assemblages as palaeoenvironmental bioindicators in late Jurassic epicontinental platforms, relation with trophic conditions. *Acta Palaeontol Pol* 53:705–722
- Reolid M, Sebane A, Rodríguez-Tovar FJ, Marok A (2012) Foraminiferal morphogroups as a tool to approach the Toarcian Anoxic event in the Western Saharan Atlas (Algeria). *Palaeogeogr Palaeoclimatol Palaeoecol* 323–325:87–99
- Reolid M, Chakiri S, Bejjaji Z (2013) Adaptive strategies of the Toarcian benthic foraminiferal assemblages from the Middle Atlas (Morocco): palaeoecological implications. *J Afr Earth Sci* 84:1–12
- Reolid M, Sánchez-Quiñónez C, Alegret L, Molina E (2015) Palaeoenvironmental turnover across the Cenomanian–Turonian transition in Oued Bahloul, Tunisia: Foraminifera and geochemical proxies. *Palaeogeogr Palaeoclimatol Palaeoecol* 417:491–510
- Reolid M, Duarte LV, Rita P (2019) Changes in foraminiferal assemblages and environmental conditions during the T-OAE (Early Jurassic) in the northern Lusitanian Basin, Portugal. *Palaeogeogr Palaeoclimatol Palaeoecol* 520:30–43
- Rhoads DC, Speden IG, Waage KM (1972) Trophic group analysis of Upper Cretaceous (Maestrichtian) bivalve assemblages from South Dakota. *AAPG Bull* 56(6):1100–1113
- Riegraf W (1985) Mikrofauna, Biostratigraphie und Fazies im unteren Toarcium Südwestdeutschlands und Vergleiche mit benachbarten Gebieten. *Tübinger Mikropaläontologische Mitteilungen* 3:1–232
- Riegraf W, Luterbacher H (1989) Upper Jurassic foraminifera of the North and South Atlantic Deep Sea Drilling Project Leg 1–79. *Geol Rundsch* 78:999–1045
- Rita P, Reolid M, Duarte LV (2016) Benthic foraminiferal assemblages record major environmental perturbations during the late Pliensbachian–early Toarcian interval in the Peniche GSSP, Portugal. *Palaeogeogr Palaeoclimatol Palaeoecol* 454:267–281
- Roy P, Bardhan S, Mitra A, Jana SK (2007) New Bathonian (Middle Jurassic) ammonite assemblages from Kutch, India. *J Asian Earth Sci* 30:629–651
- Sagasti G, Ballent S (2002) Microfaunal features of a marine transgression: the Agrio Formation 5(lower cretaceous), Neuquen Basin. *Argentina Geobios* 3(6):721–734
- Samson Y (2001) Foraminifères et reconstitution des variations bathymétriques, exemple du Kimméridgien de la région du Havre (Seine–Maritime, Normandie, France). *Rev Micropaleontol* 44:59–91
- Schafer CT, Collins ES, Smith JN (1991) Relationship of foraminifera and thecamoebian distributions to sediments contaminated by pulp mill effluent: Saguenay Fiord, Quebec. *Can Mar Micropaleontol* 17(3–4):255–283
- Seidenkrantz M-S (1993) Benthic foraminiferal and stable isotope evidence for a “Younger Dryas–style” cold spell at the Saalian–Eemian transition, Denmark. *Palaeogeogr Palaeoclimatol Palaeoecol* 102:103–120
- Sen Gupta B, Machain M (1993) Benthic foraminifera in oxygen-poor habitats. *Mar Micropaleontol* 20(3):183–201
- Sen Gupta B, Lobegeier MK, Smith LE (2003) Foraminifera of deep-bathyal and abyssal hydrocarbon seeps, Gulf of Mexico. In *Geological Society of America, Abstracts with Programs* 35: 287
- Setoyama E, Kaminski MA, Tyszka J (2011) The late cretaceous–early Paleocene palaeobathymetric trends in the southwestern Barents Sea—palaeoenvironmental implications of benthic foraminiferal assemblage analysis. *Palaeogeogr Palaeoclimatol Palaeoecol* 307:44–58

- Springer EG, Rasmussen JA, Stemmerik L (2016) Distribution and significance of foraminiferal biofacies on an aphotic Danian bryozoan mound, Karlstrup, Denmark. *Bull Geol Soc Den* 64:57–67
- Stam B (1985) Quantitative analysis of Middle and late Jurassic foraminifera from Portugal and its implications for the Grand Banks of Newfoundland. *Utrecht Micropaleontol Bull* 34:1–168
- Stam B (1986) Quantitative analysis of middle and late Jurassic foraminifera from Portugal and its implications for the Grand Banks of Newfoundland. *Utrecht Micropaleontological Bulletins* 34, 168
- Talib A, Bhalla SN (2006) Composition and age of the foraminiferal assemblage from Chari Formation, Jhurio hill, Kutch, Indian. *J Pet Geol* 15:67–81
- Talib A, Faisal SMS (2007) On the occurrence of microfossils (Foraminiferida) in the Jurassic rocks of Ler Dome, Kutch Mainland, Gujarat. *Curr Sci* 92:1–2
- Talib A, Gaur KN, Bhalla S (2007) Callovian-Oxfordian boundary in Kutch Mainland, India—a foraminiferal approach. *Rev Paléobiol* 26:625–630
- Talib A, Gaur KN, Singh YP, Wasim SM, Anjum S (2012a) Some foraminiferal taxa in the middle to Late Jurassic Sediments of Kaiya Dome, Kutch. *J Geol Soc India* 79:161–168
- Talib A, Gaur KN, Sisodia AK, Bhatt BA, Irshad R (2012b) Foraminifera from Jurassic Sediments of Keera Dome, Kutch. *J Geol Soc India* 80:667–675
- Talib A, Wasim SM, Sabeena Arkan M (2016) Jurassic foraminifera from the Dharang member, Habo formation, Habo dome, Kutch, India: systematics, age, palaeoecology and palaeobiogeography. *J Syst Paleontol* 15:403–426
- Talib A, Jain S, Irshad R (2017) Integrated benthic foraminiferal and ammonite biostratigraphy of middle to late Jurassic Sediments of Keera Dome, Kachchh, Western India. In: Kathal PK, Nigam R, Talib A (eds) *Advanced micropaleontology*. Scientific Publishers, pp 71–81
- Ter Braak CJ, Verdonschot PF (1995) Canonical correspondence analysis and related multivariate methods in aquatic ecology. *Aquat Sci* 57(3):255–289
- Tyszka J (1994a) Response of Middle Jurassic benthic foraminiferal morphogroups to dysoxic/anoxic conditions in the Pieniny Klippen Basin, Polish Carpathians. *Palaeogeogr Palaeoclimatol Palaeoecol* 110(1–2):55–81
- Tyszka J (1994b) Paleoenvironmental implications from ichnological and microfaunal analyses of Bajocian spotty carbonates, Pieniny Klippen Belt, Polish Carpathians. *Palaios* 9:175–187
- Tyszka J (1995) Mid-Jurassic palaeoenvironment and benthic communities in the Pieniny Klippen Belt and the Magura basins, Pieniny Klippen Belt, Poland. Unpublished PhD thesis, Institute of Geological Sciences, Polish Academy of Sciences, Kraków
- Van Der Zwaan GJ, Duijnste IAP, Den Dulk M, Ernst SR, Jannink NT, Kouwenhoven TJ (1999) Benthic foraminifers: proxies or problems? A review of paleoecological concepts. *Earth-Sci Rev* 46:213–236
- Wasim SM, Reolid M, Talib A, Alvi SH (2020) Callovian to Oxfordian benthic foraminifera from Ler Dome, Kutch Basin (Gujarat, India): systematic, ecostratigraphy and palaeoenvironmental reconstruction. *Riv Ital Paleontol Stratigr* 126(2):315–362
- Wasim SM, Talib A, Alvi AH (2021) Systematics, age, paleoecology and paleobiogeography of Middle to Late Jurassic benthic foraminiferal assemblages from Jumara Dome, Kutch, Gujarat, India. *Micropaleontology* 67(1):73–104
- Wolfring F, Wagneich M (2016) A quantitative look on northwestern Tethyan foraminiferal assemblages, Campanian Nierental Formation, Austria. *Peerj* 4:e1757

Springer Nature or its licensor (e.g. a society or other partner) holds exclusive rights to this article under a publishing agreement with the author(s) or other rightsholder(s); author self-archiving of the accepted manuscript version of this article is solely governed by the terms of such publishing agreement and applicable law.